PLACE IN RETURN BOX to remove this checkout from your record.

TO AVOID FINES return on or before date due.

MAY BE RECALLED with earlier due date if requested.

DATE DUE	DATE DUE
	*
	DATE DUE

5/08 K:/Proj/Acc&Pres/CIRC/DateDue.indd

Moisture Distribution in Blister Packages

By

Satish Muthu

A THESIS

Submitted to
Michigan State University
in partial fulfillment of the requirements
for the degree of

MASTER OF SCIENCE

Chemical Engineering

2009

ABSTRACT

MOISTURE DISTRIBUTION IN BLISTER PACKAGES

By

Satish Muthu

Some blister packages are designed to protect pharmaceutical drugs from environmental factors such as moisture. Moisture uptake by anhydrous solids stored in these packages is primarily controlled by adsorption/absorption phenomena and can be predicted if the thermodynamic and transport properties of the package constituents (esp., the drug and the polymer barrier phases) are known. In this thesis, a quantitative metric for the shelf life of a blister package is developed in terms of parameters associated with individual components of the package and the environmental conditions associated with storage. The adsorption/absorption model developed herein assumes that the moisture distribution rapidly attains a pseudo-steady state profile within the polymer barrier phase and within the air gap phase. This pseudo-steady state approximation (PSSA) is justified based on an exact unsteady-state analysis of a conjugate absorption problem with linear isotherms. A commercial finite element code (COMSOL MULTIPHYSICS 3.3) was used to analyze the non-linear boundary value problem resulting from the use of a GABadsorption isotherm at the solid-product/air-gap interface. The resulting mathematical model is consistent with an earlier comprehensive experimental study of moisture uptake by blister packages containing 20 mg Deltasone® tablets (see Allen, 1994). The PSSA model provides a practical tool for estimating the shelf life of blister packages and for evaluating testing protocols.

Dedicated to My Parents, Mr. and Mrs. Muthu, who have inspired me to be what I am today.

ACKNOWLEDGEMENT

The gratification and euphoria that accompany the successful completion of a project would be incomplete without mentioning those who made it possible.

I would like to express my deep sense of gratitude and indebtedness to Professor Charles Petty for his incomparable counsel and indefatigable efforts, which were invaluable for the completion of this work. In addition, I would like to sincerely thank Professor Maria Rubino, Professor Rafael Auras, and Professor André Bénard for providing their expertise and valuable input regarding this research as well as Karuna Koppula for her help in formulating the boundary value problem and the use of COMSOL Multiphysics software.

I would like to thank the Department of Chemical Engineering and Materials Science, the Department of Mechanical Engineering, the School of Packaging, Pfizer and the National Science Foundation Industry/University Cooperative Research Center for Multiphase Transport Phenomena (NSF/ECC 0331977) for all their financial and technical support during the research

Finally, I would like to thank my parents, ma belle and friends for their unconditional love and affection that kept me going through hard times.

iv

TABLE OF CONTENTS

LIST	OF TABLES	vi
LIST	OF FIGURES	vii
LIST	OF SYMBOLS	ix
СНАР	TER 1 INTRODUCTION	1
1.1	MOTIVATION	2
1.2	BACKGROUND	3
	OBJECTIVES AND OUTLINE	
СНАР	TER 2 LITERATURE REVIEW	7
2.1	WATER ACTIVITY	8
2.2	MOISTURE SORPTION ISOTHERMS	
2.3	GAB ISOTHERMS	11
2.4	WATER ABSORPTION PHENOMENA IN THE PRODUCT PHASE	14
2.5	WATER ABSORPTION PHENOMENA IN THE POLYMER BARRIER PHASE	17
2.6	BLISTER PACKAGES	19
2.7	SHELF LIFE METRIC	22
СНАР	TER 3 MASS TRANSFER MODEL	25
3.1	Introduction: One-dimensional Mass Transfer Model	26
	ASSUMPTIONS	
3.3	Unsteady and Pseudo-Steady State Models	
3.3	PSEUDO STEADY STATE MODEL FOR THE PQI-TIME	34
3.4	LINEAR ADSORPTION – ANALYTICAL SOLUTION	
3.6	LINEAR ADSORPTION – NUMERICAL SOLUTION	37
3.7	UNSTEADY STATE MODEL FOR THE PQI-TIME	37
	GAB ADSORPTION - NUMERICAL SOLUTION	
3.9	PSSA MODEL WITH A GAB ISOTHERM – EXPERIMENTAL VALIDATION	42
СНАБ	TER 4 PARAMETRIC STUDIES OF THE PSEUDO-STEADY STAT	'E
ABSO	RPTION (PSSA-) MODEL	44
4.1	Introduction	45
	INPUT DATA FOR THE PSSA MODEL	
	PSSA Model Linear Isotherm.	
	PSSA MODEL (GAB ISOTHERM)	

CHAPTER 5 CONCLUSIONS	60
CHAPTER 6 RECOMMENDATIONS	64
APPENDICES	66
APPENDIX A. ONE-DIMENSIONAL DIFFUSION FOR LINEAR ADSORPTION	
ISOTHERMS	67
APPENDIX B. PSEUDO-STEADY STATE ABSORPTION MODEL	71
APPENDIX C. UNSTEADY STATE CONJUGATE DIFFUSION	77
APPENDIX D. PROBLEM SETUP FOR THE NON-LINEAR PSSA MODEL	86
APPENDIX E. ABSORPTION: FLAT PLATE GEOMETRY AND LARGE BIOT NUM	
	90
APPENDIX F. Justification of PSSA-Model for Linear Adsorption	
REFERENCES	100

LIST OF TABLES

Table 4.1	Data used in the PSSA Model Calculations	46
Table 4.2	Groups of the PSSA Model (Linear Isotherm)	47
Table 4.3	Eigenvalues and Fourier Coefficients for the Pseudo-Steady State Model	48
Table 4.4	Eigenvalues and Fourier Coefficients for Linear Conjugate Absorption	50
Table B.1	Eigenvalues and Fourier Coefficients for the Linear PSSA-Model for $\alpha = 0.1$	74
Table B.2	Eigenvalues and Fourier Coefficients for the Linear PSSA-Model for $\alpha = 0.2$	75
Table B.3	Eigenvalues and Fourier Coefficients for the Linear PSSA-Model for $\alpha = 0.3$	76
Table F.1	Effect of the parameters N_S , N_P & N_{τ} on the PQI-time	99

LIST OF FIGURES

Figure 2.1	Classification of Adsorption Isotherms9
Figure 2.2	GAB Moisture Sorption Isotherm15
Figure 2.3	Verification of the Product Diffusion Coefficient
Figure 2.4	Verification of the Polymer Diffusion Coefficient – PVC20
Figure 2.5	Verification of the Polymer Diffusion Coefficient – Aclar21
Figure 3.1	Schematic of a Blister Package and Coordinates for the One-Dimensional Transport Model
Figure 4.1	The Effect of α on the Relaxation of the PQI-function (Linear isotherm)51
Figure 4.2	The Effect of α on the PQI-time for $\Theta_c^S = 0.5$ (Linear isotherm)52
Figure 4.3	Comparison of Experimental Results with the PSSA-model at 80% Relative Humidity (GAB isotherm)53
Figure 4.4	Comparison of Experimental Results with the PSSA-model at 90% Relative Humidity (GAB isotherm)54
Figure 4.5	Moisture Ingress as a Function of Time in the Individual Phases and in the Whole Blister
Figure 4.6	Variation of Diffusive Flux at the Product - Air Gap Interface with Time
Figure 4.7	Effect of Relative Humidity on the Moisture Sorption of a Blister Package
Figure F.1	Effect of N_{τ} on the PQI function96
Figure F.2	Effect of N _S on the PQI function97
Figure F.3	Effect of Np on the PQI function98

LIST OF SYMBOLS

NOTATION

a₁, a₂, a₃ GAB coefficients (temperature dependent).

A_n Dimensionless Fourier coefficient defined in Table 4.1.

Aw Water activity or the Relative Humidity (RH).

Bi Biot number defined by Eq.(3.9).

Bi^m Modified Biot number defined by Eq.(C.11)

CS, CG, CP, CE Concentration of water in the S-phase, G-phase, P-phase, and the

surrounding (environmental) phase, respectively (units:

mass/volume).

D_S, D_G, D_P Diffusivity of water in the S-phase, G-phase, and P-phase,

respectively (units: (length)²/time).

 F_n^S, F_n^P Eigenfunctions in the S-phase and P-phase, respectively.

k_c Convective mass transfer coefficient for water at the external PG-

interface (units: length/time).

K_{SG}, K_{PG} Thermodynamic equilibrium distribution coefficients for water

across the SG-interface and the PG interface; units: (mass of water per unit volume of S-phase)/(mass of water per unit volume of G-

phase). See Eq.(3.10).

 K_{GP}, K_{PE}

Thermodynamic equilibrium distribution coefficients across the GP-interface (between the air gap and the polymer barrier) and the PE-interface (between the polymer and surroundings). In this research $K_{GP}=K_{PG}=K_{PE}$.

 L_S, L_G, L_P

Half-thickness of the S-phase; effective gap of the G-phase, and thickness of the P-phase, respectively (units: length). See Figure 3.1.

M or M_t

Moisture content in the tablet in g / 100 g of solid tablet.

 M_{∞}

Equilibrium value of M_t.

$$N_{\tau} \equiv \sqrt{\frac{L_P^2/D_P}{L_S^2/D_S}}$$
 ... See Eq.(3.32).

$$N_S \equiv \frac{V_S K_{SG}}{V_G} \, .$$

$$N_{\mathbf{P}} \equiv \frac{V_{\mathbf{P}}K_{\mathbf{P}G}}{V_{\mathbf{G}}}.$$

PQI-

PQI = Product Quality Index. This terminology is used to designate a quantitative condition related to the moisture content of the solid product phase. The PQI-function is a volume average of the concentration difference function (see Eq.(3.15)); the PQI-time is defined by Eq.(3.7) and gives the shelf life based on a criterion for the moisture content in the product phase.

PVC Polyvinyl chloride.

RH Relative humidity of the storage environment.

S^{GP}	Mass transfer surface area between the air gap and the polymer barrier.
SSG	Mass transfer surface area included for mass transfer between the solid product phase and the air gap.
	(disk: $S^{SG} = 2\pi R^2$, $R = disk radius$)
î, t	Dimensional and dimensionless times, respectively. Time is made dimensionless by using the diffusion time scale of water in the Sphase (see Eq.(3.3)).
\hat{t}_c, t_c	Shelf life defined by Eqs.(3.7) and (3.8).
\hat{X}, X	Dimensional and dimensionless spatial position variables
	(see Figure 3.1).
\hat{x}_G, x_G	Embedded coordinate in the G-phase.
\hat{x}_S, x_S	Embedded coordinate in the S-phase.
\hat{X}_{P}, X_{P}	Embedded coordinate in the P-phase.
$\underline{\hat{\mathbf{x}}} \leftrightarrow (\hat{\mathbf{x}}_1, \hat{\mathbf{x}}_2, \hat{\mathbf{x}}_3)$	Spatial position vector in a three dimensional space.
VS	Volume of the solid product phase.
V^{G}	Volume of the G-phase.
$V^{\mathbf{P}}$	Volume of the P-phase.

-	`			
(T	re	P	k

λ_n	Dimensionless eigenvalue associated with the pseudo-steady state model (see Eq.(3.16) and (3.17) and Table 4.2).	
$\Theta^{S},\Theta^{G},\Theta^{P}$	Dimensionless concentration difference functions associated with the S-phase, the G-phase, and the P-phase, respectively (see Eqs.(3.12)-(3.14).	
$\Theta_{\mathbf{c}}^{\mathbf{S}}$	Value of the PQI-function at the critical moisture concentration (see Eq.(3.7). This dimensionless specification depends on three factors: 1) the critical moisture content of the S-phase; 2) the initial moisture content of the S-phase; and, 3) the equilibrium moisture content of the S-phase consistent with the storage conditions.	
$<\Theta^{S}>(t)$	Volume average of the water concentration difference function over the S-phase.	
ρS	Density of the tablet	
Operators and Functions		
$\hat{\nabla}^2$	Laplacian operator	
$\Im(\lambda_n)$	Function defined by Eq.(3.41). The zeros of this function correspond to the eigenvalues that appear in Eq.(3.38).	
<.>	Volume average operation associated with the S-phase (see Eq.(3.2) and Eq.(3.15)).	
$\cos(\lambda_n X)$	Eigenfunction associated with the pseudo-steady state model	

$$\frac{\partial}{\partial t}$$
, $\frac{\partial^2}{\partial X^2}$ First-order and second-order partial differential operators

Symbols, super/subscripts

- Used to designate a critical condition associated with the maximum allowable water concentration in the solid product phase (S-phase). Also used to designate a convective mass transfer coefficient (see k_c above).
- o Used to designate an initial condition.
- n Index integer for the discrete eigenvalues (n = 1,2,3,...)
- S, G, P Used to designate a property associated with the S-phase, the internal or external G-phases, and the P-phase.
- ^ Used to designate a dimensional property, or variable.
- ∞ Used to designate an equilibrium steady-state condition.

CHAPTER 1 INTRODUCTION

1.1 Motivation

Moisture protection is one of the most important functions of a blister package containing a pharmaceutical drug inasmuch as the interaction between some drugs and small amounts of water may cause physical and chemical modifications during storage (Labuza, 1985; Ahlneck.and Zografi, 1990; Bell and Labuza, 2000). Presently, extensive long-time empirical testing is used to identify optimal package designs. This research is partly motivated by the promise that a mathematical model for the shelf life of a blister package can complement current testing protocols by reducing the design cycle time for selecting package components and by providing additional assurances that FDA standards will be met by the final package design (PQRI, 2005).

The amount of moisture absorbed by drugs and excipients affects the flow, compression characteristics, and hardness of granules and tablets. Most significantly, the active form of the drug may interact with water to form undesirable products and loss of drug benefit. In addition, moisture may affect the dissolution and transport of the drug from the tablet. To avoid packaging failures, an overprotective package could be used, but this is expensive. Instead, blister packages are often tested to identify low cost options with sufficient barrier protection. However, the estimation of shelf life by experimental methods alone is laborious and is constrained by both time and cost. A suitable alternative is to use an appropriate mathematical model to predict the *long-time* absorption rates of a blister package based on mass transfer principles. Absorption experiments under extreme conditions, which would be relatively fast and cost effective, can be used to determine the thermodynamic and transport properties of specific blister

constituents. This experimental/mathematical approach should reduce the cost and time involved in shelf life estimation by eliminating repetitive and unnecessary tests. A mechanistic mathematical model could also be used to optimize the size and shape of blister packages as well as the selection and design of polymeric moisture barriers for specific applications.

1.2 Background

Moisture is an important factor in determining the shelf life of some products packaged in so-called "blisters" (see Labuza, 1985; Yoon, 2003; PQRI, 2005). In general, the shelf life of a moisture sensitive drug (or food) is primarily determined by 1) the manufacturing and packaging processes; 2) the storage environment; 3) the water sensitivity of the product; 4) the thermodynamic and transport properties of water in the constituent phases; and, 5) the design of the package. When the volume average moisture concentration of the product phase exceeds a pre-determined critical level, the blister package is removed from the shelf.

This master thesis research relates to previous studies on the shelf life of moisture sensitive products conducted at Michigan State University by Kim (1992), Allen (1994), Kim et al. (1998), and Yoon (2003) in the School of Packaging. Earlier experimental and theoretical research by Zografi et al. (1988), Howsmon and Peppas (1986), Anderson and Scott (1991), Smith and Peppas (1991), Marsh et al.(1999), and, Badaway et al.(2001) have also examined the impact of moisture on the shelf life of food and drug products.

1.3 Objectives and Outline

The objective of this research is to develop a quantitative measure of the shelf life of a moisture sensitive product based on unsteady-state mass transfer principles and to compare the model predictions with previously reported experimental data (Allen, 1994). The focus of the research is to determine how the geometry and the physical properties of a blister package influence the shelf life of a moisture sensitive product. A mechanistic understanding of the relationship between package design and product quality may contribute to a reduction in the cost associated with testing the efficacy of different package designs.

The scope of this study is limited to a simple package configuration that justifies the use of a classical one-dimensional diffusion model (see Appendix A); however, the pseudo-steady state absorption (PSSA-) model developed in Chapter 3 (and Appendix B) can easily be extended to more complex geometries and to products with other rate limiting phenomena including chemical reactions and moisture sensitive diffusion coefficients (Philip, 1994). The need to consider explicit unsteady-state moisture transport in the drug phase was clearly demonstrated in the earlier study by Kim (1992; also see Kim et al., 1998). Many shelf life prediction models for drug and food products have been proposed in the literature over the past thirty five years. A few noteworthy references are Labuza et al., 1972, Khanna and Peppas, 1978; Peppas and Khanna, 1980; Peppas and Sekhon,1980; Peppas and Kline, 1985; Khanna and Peppas, 1982; Peppas and Kline, 1985; Howsmon and Peppas, 1986; Smith. and Peppas ,1991; Anderson and Scott, 1991; and, Badawy et al., 2001.

In Chapter 3, a quantitative definition of the shelf life of a moisture sensitive pharmaceutical tablet within a blister package is defined. A mathematical model for this metric is developed based on the idea that a pseudo-steady state profile within the polymer barrier phase occurs on a time scale which is small compared with the rate of absorption by the product phase (Bischoff, 1963; Bischoff, 1965; Bowen, 1965; Hill, 1984). In the PSSA-model, the transport of water through the tablet – blister system is assumed to be governed by unsteady-state Fickian diffusion with a constant diffusion coefficient. A pseudo-steady-state diffusion model in the polymer and air gap phases together with an unsteady-state diffusion model in the product phase provides a means to determine the long-time absorption rates and, thereby, the shelf-life of a blister package. In Appendix F, conditions that support the validity of the PSSA-model for linear isotherms are identified by using an exact solution to an unsteady-state conjugate boundary value problem for moisture transport through the polymer barrier and the drug product (see Appendix C). The PSSA-model provides a conservative, albeit realistic, estimate for the shelf life of a blister package (i.e., the shelf life predicted by the PSSAmodel will be less than the shelf life predicted by the unsteady state conjugate mass transfer problem. Therefore, the proposed approach developed hereinafter provides a practical means for screening design options.

The PSSA-model is comprehensive in the sense that it incorporates all the physical and environmental parameters that influence the shelf life of a blister package. Model predictions are used to interpret previously published experimental data for blister packages by Allen (1994). Selected experimental data from Allen's work were used to

confirm the thermodynamic and transport properties for individual components of the blister package. This information defines a benchmark for a parametric study of the PSSA-model in Chapter 4. The parametric results provide a basis to further develop a strategy for improving the design of blister packages for moisture sensitive pills.

CHAPTER 2 LITERATURE REVIEW

2.1 Water activity

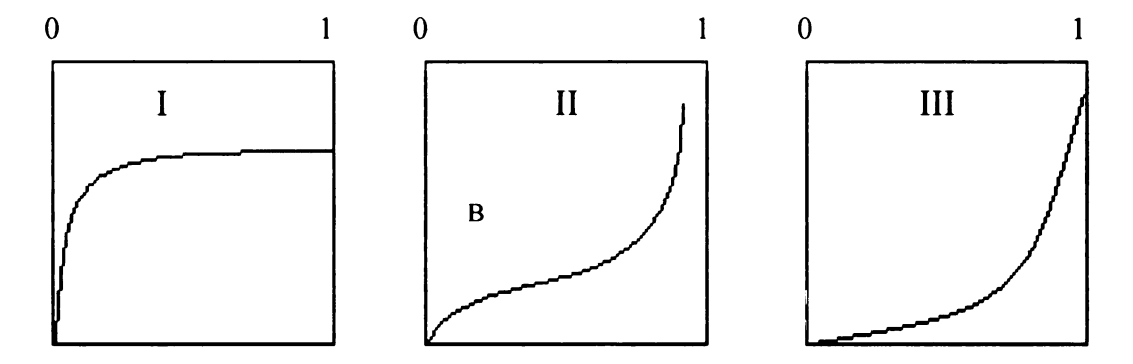
Water activity is a measure of the relative availability of water to hydrate a material. The water activity is related to the chemical potential of the system by the thermodynamic relation (Van den Berg and Bruin, 1981):

$$\mu = \mu_0 + RT \ln (f/f_0)$$
 (2.1)

In the above equation, μ (J/mole) is the chemical potential of the system; μ_0 is the chemical potential of the pure substance at temperature T (O K); R is the gas constant; and, f is the fugacity or the escaping tendency of a substance. The parameter f_0 is the escaping tendency of the anhydrous material. The water activity of a substance is defined as f/f_0 and is designated as A_W ($\equiv f/f_0$). For all practical purposes involving the conditions under which blister packages are found, the fugacity is approximately equal to the relative vapor pressure, (i.e., $A_W = f/f_0 \cong p/p_0$). Thus, the relative humidity and the water activity are equal and can be calculated as the ratio of the vapor pressure of water in air to the saturation vapor pressure. Clearly, the temperature and the relative humidity (water activity) of the surrounding humid air will influence the quality of food and drug products (Rockland and Stewart, 1981).

2.2 Moisture Sorption Isotherms

As illustrated by Figure 2.1, moisture sorption isotherms can be classified into six major types (IUPAC, 1985). When the surface coverage is sufficiently low all the isotherms reduce to a linear form referred to as the Henry's law region. The Type I



Six different adsorption isotherms for a solid/air interface. M represents the mass of water adsorbed per unit mass of dry solid and A_W represents the relative humidity, which increases from 0.0 (dry) to 1.0 (100%).

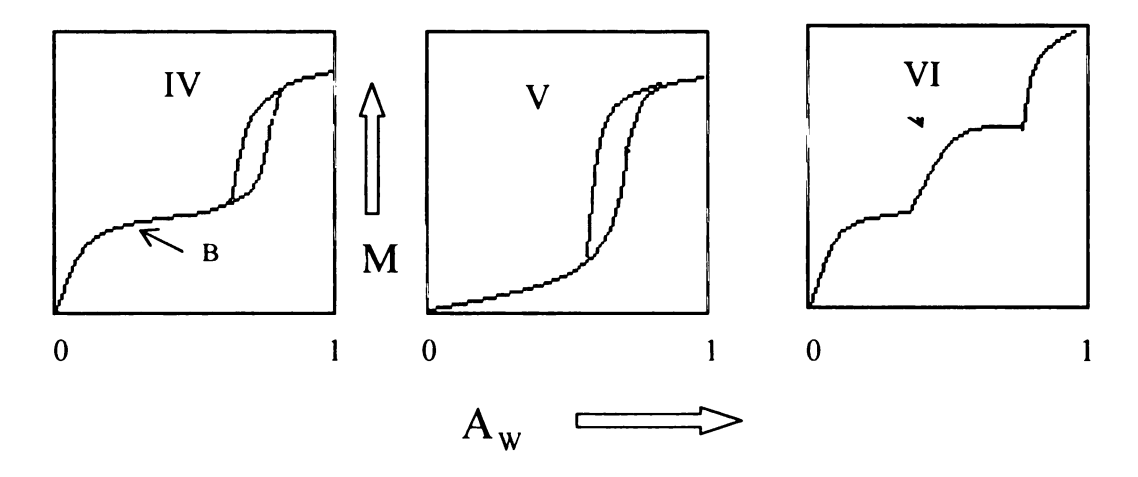


Figure 2.1 Classification of Adsorption Isotherms (IUPAC, 1985).

isotherm is reversible and is concave to the A_W (i.e., p/p_0) axis. The amount adsorbed (i.e., number of molecules or moles per unit area) approaches a finite value as the activity tends towards unity. Type I isotherms are sometimes referred to as *Langmuir isotherms*. This type of behavior occurs for microporous solids that have relatively small external surface areas (such as activated carbons and zeolites). Pores with diameters larger than 50 nm are called macropores; pores with diameters between 2 nm and 50 nm are called mesopores; and, pores with diameters less than 2 nm are called micropores.

The Type II isotherm, which is commonly encountered, is also reversible. Most adsorbents, which are non-porous (or macroporous), exhibit this kind of behavior. These isotherms exhibit monolayer-multilayer adsorption phenomena. Point B on Figure 2.1 represents the onset of multilayer adsorption phenomena. Type III isotherms are convex over the entire range of A_W and, thereby, do not show a distinct Point B. This type of isotherm is not very common but few systems like nitrogen on polyethylene show this type of behavior.

Type IV isotherms show adsorption/desorption hysteresis due to capillary condensation occurring within the mesopores at the interface and the limited uptake over a range of high A_W. The Type IV isotherm is similar to the Type II isotherm for small values of A_W. Many mesoporous industrial adsorbents exhibit this type of behavior. Type V isotherms are similar to the Type III isotherms. It has weak adsorbent/adsorbate interaction similar to the Type II isotherm, but is distinguished by the fact that it has a hysteresis loop. Type VI isotherms, which are characteristics of non-porous surfaces

show step-wise multilayer adsorption phenomena. The height of each step represents the monolayer capacity of each adsorbed layer. The sharpness of each step is dependent on the system chosen and the ambient temperature. Type VI behavior is exemplified by argon (or krypton) on graphitized carbon black at liquid nitrogen temperatures.

2.3 GAB Isotherms

In spite of its limitations, the classical Brunauer, Emmett and Teller (BET-) multilayer sorption equation is still used to calculate monolayer values under different physicochemical conditions (Perry and Green, 1997). From these data, specific area values are obtained. It is mainly used because of the simplicity of its application and because it has the approval of the International Union of Pure and Applied Chemistry (IUPAC, 1985). A 1985 report by the Commission on Colloid and Surface Chemistry recommends that the BET isotherm be used as a standard for monolayer adsorption for A_w in the range: $0.05 < A_W < 0.3$. Multilayer sorption isotherms show a sigmoid, or S-shaped, form and are well represented by the BET-isotherm defined by

$$v = \frac{v_{\text{mB}} c_{\text{B}} A_{\text{W}}}{(1 - A_{\text{W}})(1 + (c_{\text{B}} - 1) A_{\text{W}})}.$$
 (2.2)

In the above equation, v represents the amount of water (sorbate) adsorbed by a gram of sorbant if the water activity of the humid air at the interface is A_W . The parameter v_{mB} represents the monolayer value in the same units as v and the constant c_B is the difference in the free enthalpy (standard chemical potential) of the sorbate molecules in the pure liquid state and in the monolayer (first sorbed) state. To obtain the two characteristic constants from experimental data, the BET equation is often rewritten as

$$F_{BET} = \frac{A_W}{(1 - A_W)v} = \frac{1}{c_B v_{mB}} + \frac{c_B - 1}{c_B v_{mB}} A_W.$$
 (2.3)

If the BET-postulate is valid, then a plot of F_{BET} vs. A_W is linear. This usually occurs at low activities (0.05 < A_W < 0.3). For A_W > 0.3, an upward curvature is observed for F_{BET} . This deviation shows that, at higher activities, less gas or vapor is sorbed than that anticipated by the BET-equation based on constants deduced from low activity data (i.e., the parameter v is weakly dependent on A_w for A_w > 0.3).

The Guggenheim, Andersen and de Boer (GAB-) sorption equation has a similar structure as the BET-isotherm (Anderson , 1946). This equation is often employed to account for deviations from the classical BET isotherm (Costantino et al. 1997; Moreira et al., 2002; Moreira et al., 2003). The main reason for its use is that the activity range covered by this isotherm is much wider than that of the BET-equation ($0.05 < A_W < 0.8 - 0.9$). In other fields, the use of the GAB-isotherm is not well established. The GAB-isotherm is defined by

$$v = \frac{v_{mG} c_{G} k A_{W}}{(1 - kA_{W})(1 + (c_{G} - 1)k A_{W})}.$$
(2.4)

Here v_{mG} is the GAB-monolayer capacity and c_{G} is the analogue of the BET energy coefficient c_{B} . The GAB-model assumes that sorption states of the water molecules in the layers beyond the first are the same, but different from the pure liquid state. This idea requires the introduction of an additional coefficient, k. This constant is a measure of the difference of free enthalpy (standard chemical potential) of the sorbate molecules in these two states (i.e., the pure liquid state and the second sorption stage above the monolayer).

Likewise, the other GAB-energy constant measures the difference of the chemical potentials of the sorbate molecule in the upper sorption layers and in the monolayer. The GAB-isotherm can be rewritten as

$$F_{GAB} = \frac{A_W}{(1 - k A_W)v} = \frac{1}{c_G k v_{mG}} + \frac{c_G - 1}{c_G v_{mG}} A_W.$$
 (2.5)

With k=1, the GAB-isotherm reduces to the original BET equation $(v_{mB}=v_{mG};c_{B}=c_{G}).$

Eq.(2.4) can also be rewritten as

$$M = \frac{v}{v_{mG}} = \frac{A_{W}}{a_{3} A_{W}^{2} + a_{2} A_{W} + a_{1}},$$
(2.6)

which is used in this study (see Chapter 3) to account for the adsorption of water by the solid drug phase. Also see Kim (1992), Allen (1994) and Kim et al. (1998). In Eq.(2.6), the parameter M represents the mass of water adsorbed relative to the mass of solid. The coefficients a_1, a_2 , and a_3 are related to the GAB parameters by the following equations:

$$a_{1} = \frac{1}{c_{G}k}$$

$$a_{2} = \frac{c_{G} - 2}{c_{G}k}$$

$$a_{3} = -\frac{(c_{G} - 1)k^{2}}{c_{G}k}$$

$$(2.7a,b,c)$$

Note that

$$a_1 + a_2 + a_3 = \frac{(c_G - 1)}{c_G} \frac{(1 - k^2)}{k}$$
 (2.8)

Generally, $c_G \ge 1$ and $k \le 1$. These parameters depend on the temperature and the specific properties of the solid phase. It is noteworthy that for $c_G > 1$ and $k \to 1$, the GAB isotherm approaches the BET isotherm and $M \to \infty$ for $A_W \to 1$ (see Type II isotherm in Figure 2.1 above). For $c_G \ge 1$ and $k \le 1$, $M \to M_C < \infty$ for $A_W \to 1$ (see Type III isotherm in Figure 2.1 above).

Figure 2.2 illustrates the GAB-isotherm for 20 mg Deltasone® tablets at room temperature. Deltasone® is a brand of prednisone, which is used for anti-inflammatory purposes in the treatment of arthritis. The following GAB parameters,

$$a_1 = 0.064$$
, $a_2 = 1.922$, and $a_3 = -1.79$,

were measured by Allen (1994) and were used in the modeling study reported by Kim et al. (1998). Figure 2.2 shows that the linear isotherm based on the GAB-parameter a_1 significantly over predicts the concentration of moisture at the solid/air interface for $A_W > 0.03$.

2.4 Water Absorption Phenomena in the Product Phase

Water absorption by solid materials (esp., pharmaceutical drugs) surrounding by humid air involves two steps: 1) water adsorption onto the surface; and, 2) subsequent diffusion of water through the solid phase. Moisture adsorption is characterized by a sorption isotherm. The use of an isotherm at the solid/gas interface assumes that the solid interface is in thermodynamic equilibrium with the contiguous gas phase. The isotherm is an algebraic (usually non-linear) equation that relates the concentration of moisture at the

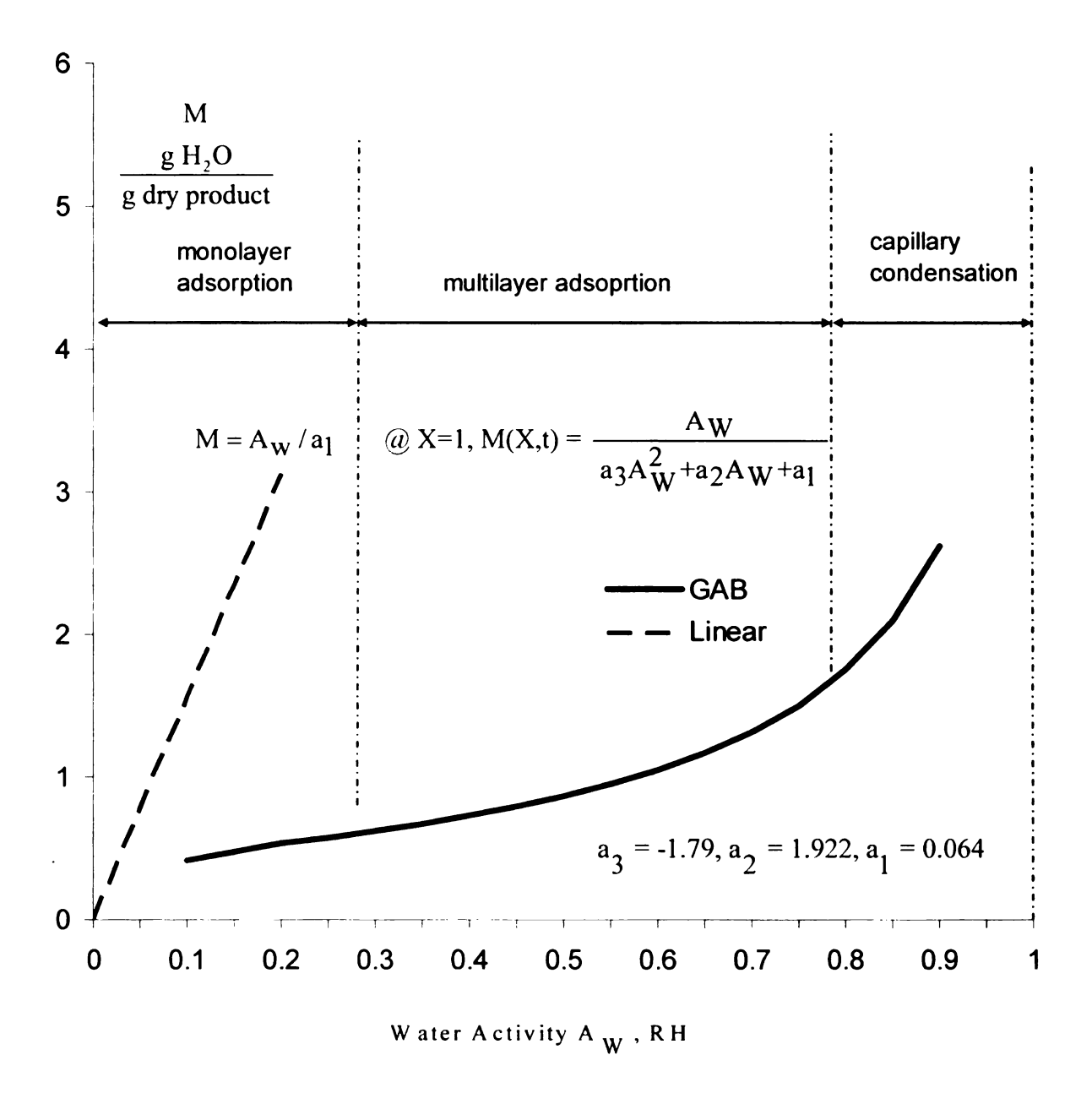


Figure 2.2 GAB Moisture Adsorption Isotherm.

surface in the solid product phase to the concentration of moisture at the surface in the adjacent gas phase. During the absorption process, the concentration at the interface changes with time until an equilibrium is established between the bulk solid and bulk gasphases. Local equilibrium at the interface occurs instantaneously, but equilibrium between the bulk phases may require years, depending on the governing transport phenomena.

Various mathematical equations have been reported in the literature to account for moisture sorption phenomena in food and in pharmaceutical products (see, esp., Labuza et al., 1972, Khanna and Peppas, 1978; Peppas and Khanna, 1980; Peppas and Sekhon,1980; Peppas and Kline, 1985; Khanna and Peppas, 1982; Peppas and Kline, 1985; Howsmon and Peppas, 1986; Smith. and Peppas, 1991; Anderson and Scott, 1991; Masaro and Zhu, 1999; and, Badawy et al., 2001). Diffusion through the solid product phase is by gradient diffusion with a diffusion coefficient that may depend on the local thermodynamic state (i.e., temperature and moisture concentration). Earlier sorption models (for porous solids) assumed that the moisture content of the solid phase quickly adjusted to the moisture content of the surroundings and that shelf-life was primarily controlled by external resistance to mass transfer. Over the past twenty years, a significant amount of work has emphasized physicochemical phenomena associated with the solid product phase (see, esp., Allen, 1994, Kim et al., 1998).

Allen measured the diffusion coefficient and the adsorption coefficients for Deltasone® tablets. The one dimensional boundary value problem for the tablet (i.e., flat

plate geometry) surrounded by humid air at constant concentration is described in Appendix E. The boundary value problem was solved analytically by using standard separation-of-variable techniques (see, Rice and Do, 1995; Bird et al., 2002) and computationally by using a commercial PDF solver based on a finite element method (COMSOL MULTIPHYSICS®). Allen used the results from Crank (1975) to estimate the diffusion coefficients from the experimental data. For the analogous heat transfer problem, see the classical paper by Gurney and Lurie (1923). Figure 2.3 compares the theoretical prediction of the volume average moisture concentration with the experimental data reported by Allen (1994). The characteristic diffusion time for the solid phase, $L_{\rm S}^2/D_{\rm S}$, is about 11 hours. The thermodynamic and transport properties of Deltasone® tablets measured by Allen will be used as a reference case for the parametric study summarized in Chapter 4.

2.5 Water Absorption Phenomena in the Polymer Barrier Phase

Capillary transport and activated diffusion are the two main modes of mass transport through polymers (Brandrup et al., 1999). Capillary transport involves the passage of molecules through pinholes and/or very porous media such as cellulose and glass. Activated diffusion essentially involves three steps: the first step involves the adsorption of the diffusing species onto the non-porous polymer film; the second step involves diffusion through the film due to a concentration gradient; and, the final step involves desorption from the film surface. Thus, mass transport across the polymer barrier is controlled by adsorption, diffusion, and desorption. Diffusion can be viewed as a series of activated jumps from one cavity to another in a water matrix. The rate of

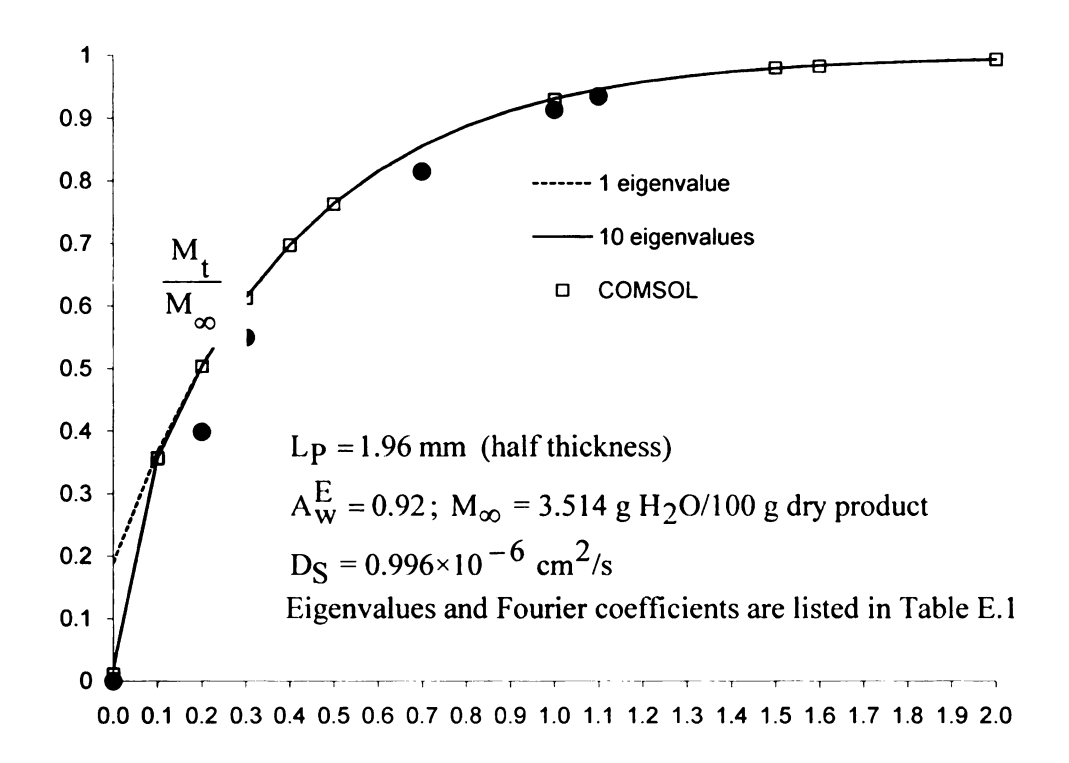


Figure 2.3 Absorption of Water by Deltasone® Tablets at Room Temperature.

t

diffusion is proportional to the number of cavities in a polymeric film. The presence of a plasticizer increases the diffusivity; crystalline polymer structures tend to decrease the diffusivity.

The polymeric film used by Allen (1994) was a composite of two polymers: PVC and ACLAR®. The diffusion coefficients for both polymers were measured in the same fashion as the pharmaceutical product by measuring the moisture uptake in the presence of humid air. The rate data were used to estimate the diffusion coefficient. The diffusion coefficients for both polymers were reported by Allen (1994) and verified in this study by using the analysis briefly described in Appendix E. Figures 2.4 and 2.5 illustrate the comparison between the experimental observations and the theoretical results.

2.6 Blister Packages

The stability, physical condition and potency of a drug tablet may be threatened by exposure to moisture, heat, oxygen and light. Many drugs, such as penicillin, are completely inactivated by exposure to moisture. Clearly, a well designed package is an essential step in the distribution and use of these products. Typical barrier strategies commonly employed in packaging include impenetrable moisture barriers (aluminum), coated product pills, and permeable plastic films. Barrier polymer films or plastics can be used to produce clear pre-formed plastic packages, which are shaped like a blister. These blister packs store the drug pills and are sealed at the open end with metal foils such as aluminum. Blister packs are also known as push through packs in some parts of the world, because of the technique used to remove the tablet from the blister pack. Blister packages

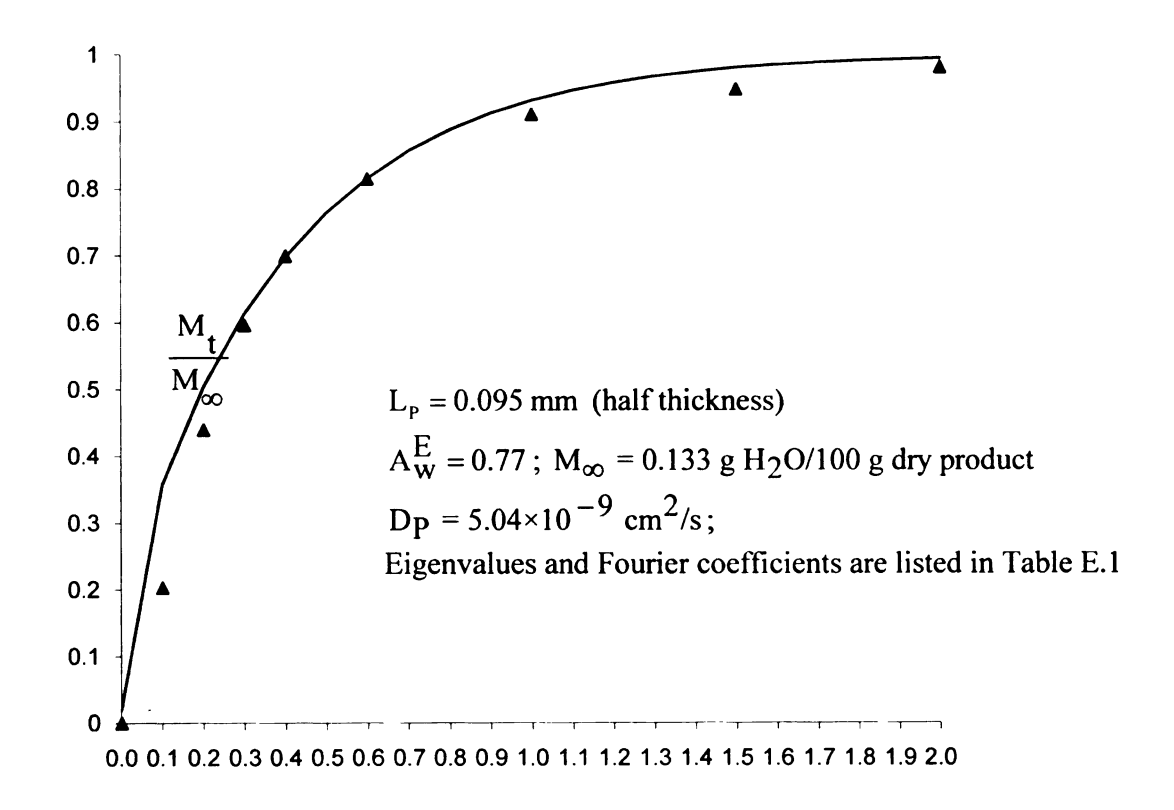
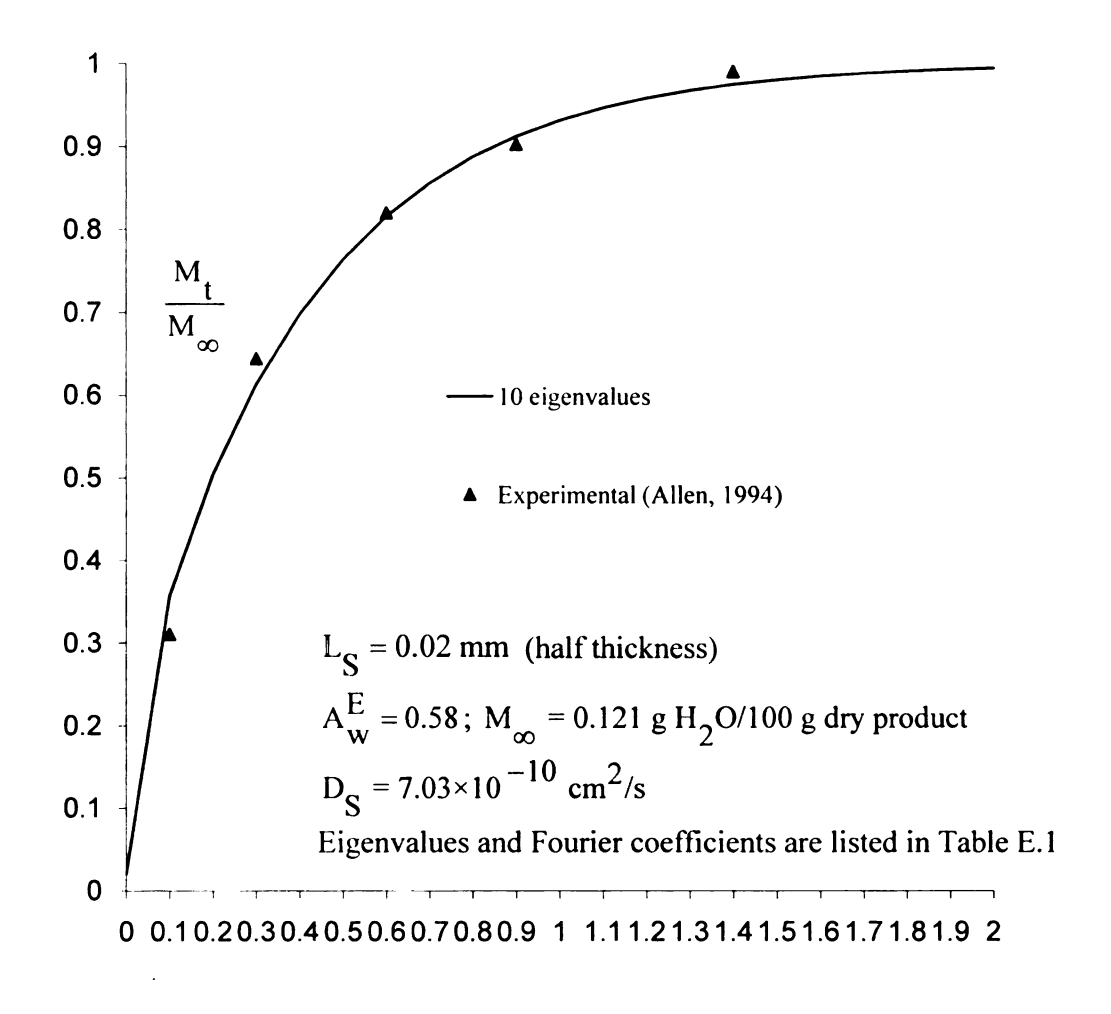


Figure 2.4 Absorption of Water by PVC Film at Room Temperature.

t



t

Figure 2.5 Absorption of Water by ACLAR® Film at Room Temperature

have several advantages inasmuch as they prevent cross contamination of the drugs at various stages and they reduce abrasion of the tablets during distribution. Blister packages also reduce the chance of overdose for over-the-counter drugs by printing the days of the week above the dose. They also save storage space compared to bottles.

Blister packs are hard to be tampered with, and the transparency of the polymer films ensures easy identification of the drug tablet. Figure 2.6 illustrates the idea of a blister package for a drug tablet.

2.7 Shelf Life Metric

Water is a main component of many pharmaceutical products and hence it plays an important role in determining their physical and chemical properties. Water controls mass transfer rates, microorganism activity, and rates of various chemical reactions. Hence, the quality of a pharmaceutical product may be influenced significantly by either a gain or a loss of moisture. Drug quality is determined by the chemical reactivity of the product as a function of time and the environmental conditions. Moisture can act as a solvent and cause a dilution effect on the substrates, which in turn can lead to increased reactivity.

The shelf life of a blister package containing a moisture sensitive drug tablet (or pill) is defined as the time needed for the product phase to acquire an unacceptable volume average moisture concentration. The shelf life will depend on a number of factors including: 1) The initial moisture concentration of the product phase, the air-gap phase,

and the polymer barrier phase; 2) The temperature and the relative humidity of the surrounding (environmental) phase; 3) The thermodynamic and transport properties of the constituent phases of the blister package; and, 4) The surface area and the volume of each constituent phase (i.e., product, air-gap, and polymer barrier). The manufacturing and processing conditions will determine the initial conditions of the constituent phases and may influence the transport properties of the polymer barrier phase during thermal forming. Because of this possibility, it is important to use extreme environmental testing (i.e., short time experiments as mentioned in Section 1.1 above) to confirm the thermodynamic and transport properties of the polymer barrier. The shelf life for a blister package can be estimated empirically by simply storing packages under given conditions until the volume average moisture concentration of the drug tablet acquires an unacceptable value. Accurate estimates for the shelf life can also be made by using "accelerated testing" in combination with mathematical simulations. "Storage testing" is obviously expensive and time consuming, but this approach is presently mandated by the FDA as an integral part of a New Drug Application (see USP XXII "Stability Considerations in Dispensing Practice", Current Good Manufacturing Practice for Finished Pharmaceuticals" 21 CFR). This paradigm has also been employed for testing food packages for more than forty years (see Karel, 1967).

Allen (1992) explored the possibility of using an "accelerated testing" protocol for blister packages under extreme storage conditions of relative humidity and temperature. This high-rate absorption data can be used to evaluate the thermodynamic and transport properties of constituent phases within a blister package. A mathematical

model can then be used to predict the time required for an unacceptable condition to occur in the product phase. The prediction of shelf life at less extreme conditions based on a mathematical model clearly depends on the assumptions used to develop the model (see Section 3.2 below). Allen (1994) partially tested this strategy with an absorption model previously developed by Kim (1992). Although predictions based on the non-linear absorption model developed by Kim were not completely satisfactory (see pages 66-73 in Allen's thesis), the non-linear PSSA-model developed in Chapter 3 below provides an explanation of the blister results reported by Allen.

CHAPTER 3

MASS TRANSFER MODEL

3.1 Introduction: One-dimensional Mass Transfer Model

The moisture concentration in a drug tablet within a blister package is developed in this section based on a one-dimensional diffusion model. The model requires the specification of a single length scale for each phase. As illustrated by Figure 3.1 L_S is defined as the half-thickness of the tablet (S-phase); Lp is the thickness of the polymer barrier (P-phase); and, L_G is the thickness of the air gap (G-phase). For this geometry, the shelf life will depend on the following two geometric ratios,

$$N_1 \equiv L_G / L_S$$
 and $N_2 \equiv L_P / L_S$. (3.1a,b)

For blister packages, $N_1 < 1$ and $N_2 \square 1$.

3.2 Assumptions

The main assumptions underlying the moisture absorption models are:

- a. The product tablet can be treated as a flat plate (neglect end effects and curvature);
- b. Moisture transfer through the product phase and the polymer barrier is by Fickian diffusion. The diffusion coefficients are assumed to be constant (weak function of temperature and moisture concentration);
- c. The moisture sorption isotherms for the drug tablet and the polymer barrier are known;
- d. The temperature and the relative humidity of the surrounding environment are constant;
- e. Absence of moisture sorption/desorption hysteresis;
- f. Moisture concentration in the air-gap (G-phase) is spatially uniform, but time dependent; and,
- g. The initial conditions in the product phase, in the air-gap phase, and in the polymer barrier phase are in thermodynamic equilibrium with the humid air in the air-gap phase and the surrounding environment

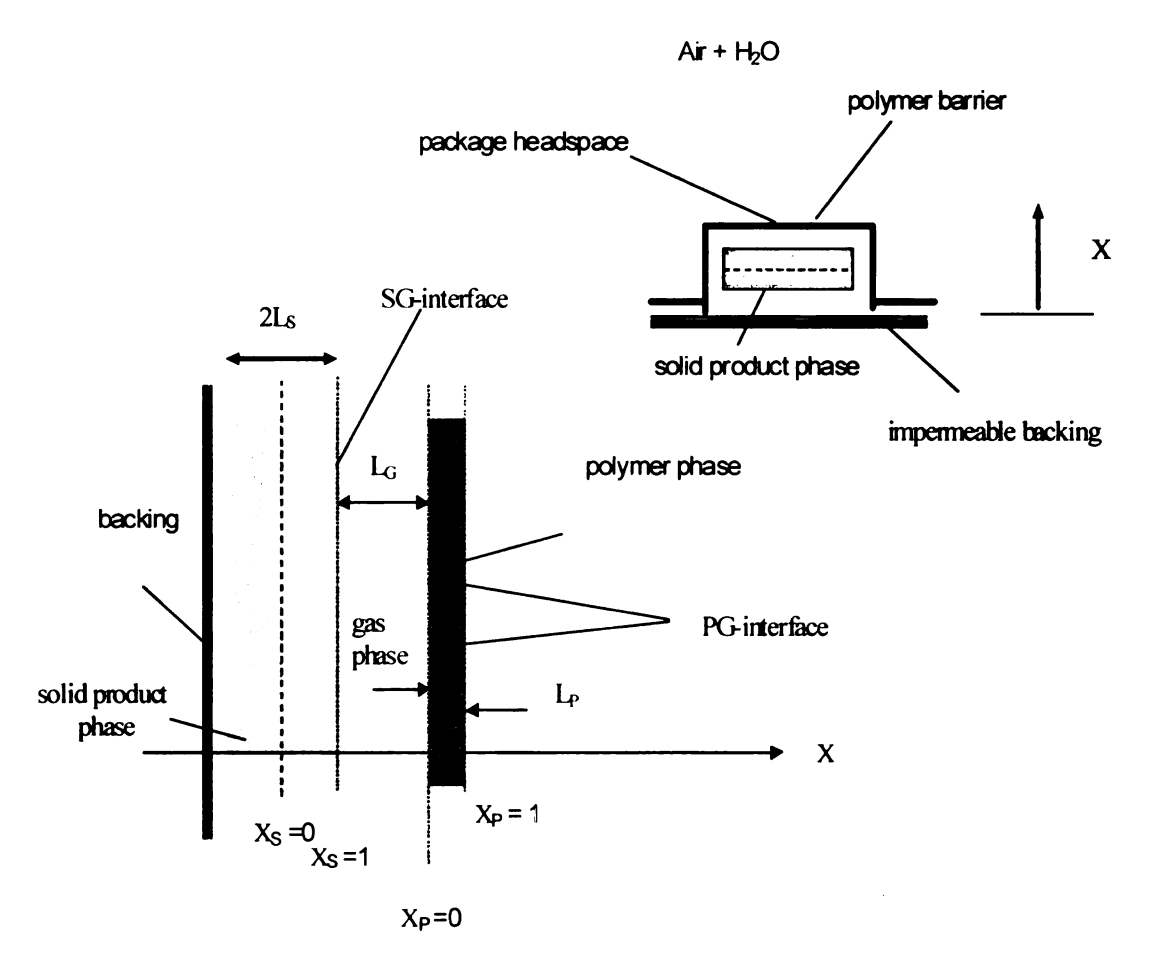


Figure 3.1 Schematic of a Blister Package for One-Dimensional Absorption.

3.3 Unsteady and Pseudo-Steady State Models

Unsteady-state absorption occurs by changing the relative humidity of the environmental phase. In this study, a Product Quality Index (PQI-) function, which incorporates the major factors that determine the shelf life of a moisture sensitive product, is defined as

$$<\Theta^{S}>(t) \equiv \frac{C_{eq}^{S} - \langle C^{S} \rangle(\hat{t})}{C_{eq}^{S} - C_{o}^{S}}.$$
 (3.2)

In the above definition, C_{eq}^S is the steady-state, equilibrium moisture concentration in the solid product phase (S-phase); C_0^S is the initial moisture concentration; and, $< C_0^S > (\hat{t})$ is the instantaneous volume average moisture concentration:

$$< C^{S} > (\hat{t}) = \frac{1}{V_{S}} \iiint C^{S}(\hat{X}, \hat{t}) dV^{S}.$$
 (3.3)

The instantaneous water concentration within the S-phase, $C^S(\hat{X},\hat{t})$, depends on the position vector \hat{X} and the time \hat{t} ; V^S denotes the volume of the S-phase. The dimensionless PQI-function depends on a dimensionless time defined by

$$t = \frac{\hat{t} D_S}{L_S^2}.$$
 (3.4)

 D_S is a constant diffusion coefficient for water in the S-phase and L_S is a characteristic length scale (half-thickness of the S-phase).

The quality of a moisture sensitive product degrades as it absorbs moisture. For t=0, the product phase has a moisture content determined by the manufacturing and packaging processes. The PQI-function is defined so that $<\Theta^S>(0)\equiv 1$. If the blister package is exposed to a humid environment not in equilibrium with its initial state, then the PQI-function relaxes to zero as time increases, $<\Theta^S>(t)\to 0$ as $t\to\infty$. Consequently, the PQI-function decreases monotonically from unity to zero,

$$0 \le <\Theta^{\mathbf{S}} > (t) \le 1 \quad , \quad 0 \le t \le \infty \,. \tag{3.5}$$

For a one-dimensional model, the PQI-time, which provides an objective metric to compare different package designs, depends on different dimensionless groups related to the shape of the package and the physical properties that control the unsteady-state absorption of water. The critical PQI-time is defined as follows

$$<\Theta^{S}>(t_{c}) = <\Theta^{S}>_{c}, 0 \le t_{c} < \infty.$$
 (3.6a)

As noted above, the parameter $<\Theta^S>_c$ depends on C_{eq}^S , $< C^S>_c$, and C_o^S . The moisture concentration of the solid product phase in equilibrium with the surrounding humid air is designated as C_{eq}^S . The critical (i.e., unacceptable) volume average moisture concentration of the solid product phase is designated as $< C^S>_c$. The initial moisture concentration of the solid phase, which is in equilibrium with the air-gap phase, is designated as C_o^S .

For moisture sensitive products, the water concentration must not exceed some critical limit, < C^S > $_c$. If the surrounding humid air leads to an equilibrium concentration of water in the product phase for which $C_{eq}^S \ge <$ C^S > $_c$, then the shelf life \hat{t}_c must be selected so that

$$C_0^S \le \langle C^S \rangle (\hat{t}) \le \langle C^S \rangle (\hat{t}_c) = \langle C^S \rangle_c \le C_{eq}^S , \quad 0 \le \hat{t} \le \hat{t}_c \le \infty.$$
 (3.6b)

Ineq. (3.6b) is equivalent to the following inequality for the PQI-function,

$$[0 = \langle \Theta^{S} \rangle (\infty)] \ \Box \ [\langle \Theta^{S} \rangle (t_{c}) \equiv \langle \Theta^{S} \rangle_{c}] \ \leq \ \langle \Theta^{S} \rangle (t) \leq \ [\langle \Theta^{S} \rangle (0) = 1]. \quad (3.6c)$$

The critical concentration < C S > $_c$ is clearly product specific and has nothing to do with either the initial moisture content of the S-phase or the humid air of the surroundings (Ahlneck and Zografi, 1990). However, as implied by Eq. (3.2), the time needed for the volume average water concentration in the S-phase to become equal to C_c^S (i.e., $<\Theta^S>_c(t_c)=<\Theta^S>_c$) does depend on C_o^S and C_{eq}^S . Therefore, if C_o^S , C_{eq}^S , and $C_o^S>_c$ are all specified, then the shelf life can be determined by solving the following equation for the PQI-time ($\equiv t_c$):

$$<\Theta^{S}>(t_{c}) \equiv \frac{C_{eq}^{S}-(\hat{t}_{c})}{C_{eq}^{S}-C_{o}^{S}} = \frac{C_{eq}^{S}-_{c}}{C_{eq}^{S}-C_{o}^{S}} \equiv <\Theta^{S}>_{c}.$$
 (3.7)

The dimensional shelf life is proportional to the PQI-time and can be expressed as

$$\hat{t}_{c} = \frac{L_{S}^{2}}{D_{S}} t_{c}. \tag{3.8}$$

Mass Transfer: Fickian Diffusion

In the approach adopted hereinafter, water is transported by ordinary diffusion with a constant diffusion coefficient in each phase. D_S , D_G , and D_P represent, respectively, the diffusivity of water in the S-phase, G-phase, and P-phase of the blister package (see Figure 3.1). The dimensionless PQI-time depends on the relative values of the diffusion coefficients:

$$N_3 \equiv D_G / D_S$$
 and $N_4 \equiv D_P / D_S$. (3.9a,b)

The diffusivity ratio N₃ is usually very large (N₃ \square 10⁴); however, N₄ << 1.

External Mass Transfer: Environmental Convection & Diffusion

The transport of water to the external surface of the blister package may be influenced by forced convection, natural convection, and multi-component diffusion phenomena (Bird et al., 2002). In this study, the simultaneous transport of oxygen and nitrogen with water is neglected. The analysis also assumes that the temperature and the total pressure of the internal and external gas phases are constant and that local heating effects due to absorption (mixing) are unimportant. In this study, a convective mass transfer coefficient $k_{\rm C}$ accounts for the resistance to mass transfer near the external surface of the blister package. Thus, the Biot number for interfacial mass transfer, defined as

$$N_5 \equiv Bi \equiv \frac{k_c L_P}{D_P} , \qquad (3.9c)$$

also influences the PQI-time. The Biot number depends on the environmental Schmidt number, $Sc \equiv v^E/D^E$, and an environmental Reynolds number, $Re \equiv \ell_c u_c/v^E$, based

on a characteristic length and velocity scale associated with the surroundings. Previous studies usually assume that $N_5 \to \infty$. Although this assumption yields the simplification that the water at the polymer/gas (PG-) interface is instantaneously at its final steady state condition, the formal analysis developed hereinafter retains the possibility that the external resistance to mass transfer may limit the rate of absorption.

Thermodynamic Equilibrium at Interfaces

The water in the S-phase near the SG-interface is assumed to be in thermodynamic equilibrium with the water in the G-phase near the SG-interface (see Figure 3.1). The local thermodynamic equilibrium assumption (see Bird et al., 2002; Rice and Do, 1995; Smith and Peppas, 1991; Kim et al., 1998) is also imposed on the PG- and GP-interfaces. In this research, the adsorption and desorption isotherms are equal (i.e. no hysteresis).

At steady state, thermodynamic equilibrium applies everywhere and the water concentration is spatially uniform in each phase. The temperature-dependent, thermodynamic distribution coefficients at the SG-interface and the PG-interface for small values of A_W (i.e., low relative humidity) are denoted as K_{SG} and K_{PG} . These two parameters, which influence the PQI-time, are used in this research to account for the discontinuity in water concentration between phases:

$$C_{S}(\hat{X}_{SG}, \hat{t}) = K_{SG} C_{G}(\hat{X}_{SG}, \hat{t}) \text{ (adsorption)}$$
(3.10a)

$$C_{P}(\hat{X}_{GP}, \hat{t}) = K_{GP} C_{G}(\hat{X}_{GP}, \hat{t}) \quad \text{(desorption)}$$
(3.10b)

$$C_{\mathbf{P}}(\hat{\mathbf{X}}_{\mathbf{PG}},\hat{\mathbf{t}}) = K_{\mathbf{PG}} C_{\mathbf{G}}(\hat{\mathbf{X}}_{\mathbf{PG}},\hat{\mathbf{t}}) \quad \text{(adsorption)}. \tag{3.10c}$$

The thermodynamic distribution coefficients K_{SG} , K_{GP} and K_{PG} are temperature dependent and could vary significantly. In general, K_{PG}/K_{SG} \square 1.

The adsorption isotherm for the drug tablet is given by the Guggenheim-Anderson-deBoer (GAB-) sorption isotherm (see Eq.(2.6) and Figure 2.2). For small values of A_w :

$$M = \frac{A_W}{a_3 A_W^2 + a_2 A_W + a_1} \xrightarrow{A_W \Box 1} \frac{1}{a_1} A_W, K_{SG} = \frac{1}{a_1}$$
 (3.10d)

In the above equation, A_W is the activity of water in the air gap phase $(0 \le A_W \le 1)$ and the dimensionless coefficients a_1 , a_2 and a_3 are the product specific GAB-parameters (temperature dependent, but independent of A_w). In summary, the dimensionless PQI-time defined by Eq.(3.7) depends on the foregoing dimensionless parameters and the critical PQI coefficient, $<\Theta^S>_c$. Thus,

$$t_{c} = F(N_{1}, N_{2}; N_{3}, N_{4}, N_{5}; K_{SG}, K_{PG}; \Theta_{c}^{S})$$
(3.11)

where N_1 and N_2 characterize the geometry of the blister package; N_3 , N_4 , and N_5 relate to relative mass transfer influences; and, K_{SG} and K_{PG} are dimensionless thermodynamic distribution coefficients.

Table 4.2 in Chapter 4 shows the range over which each of the above independent dimensionless groups may vary for blister packages. Eq. (3.11), albeit complicated, provides a means to objectively compare the performance of different blister package

designs. As demonstrated in the next section, this relationship simplifies considerably by using a pseudo-steady state approximation for the G- and P-phases.

3.3 Pseudo Steady State Model for the PQI-time

Eq.(3.11) simplifies significantly if a pseudo-steady state assumption is used to approximate the transport of water across the thin polymer barrier and the air gap (see Appendix B). The mass transfer resistance between the surroundings and the outer surface of the blister package is included in the analysis by using a convective mass transfer coefficient. Appendix A defines the initial boundary-value problem in terms of the following concentration differences between the final equilibrium water concentration and the local instantaneous water concentration in each phase:

$$\Theta^{S}(X,t) = \frac{C_{eq}^{S} - C^{S}(\hat{X},\hat{t})}{C_{eq}^{S} - C_{o}^{S}} , \quad 0 \le X_{S} \le 1$$
(3.12)

$$\Theta^{G}(X,t) = \frac{C_{eq}^{G} - C_{0}^{G}(\hat{X},\hat{t})}{C_{eq}^{G} - C_{0}^{G}} , \quad 0 \le X_{G} \le 1$$
(3.13)

$$\Theta^{P}(X,t) = \frac{C_{eq}^{P} - C_{Q}^{P}(\hat{X},\hat{t})}{C_{eq}^{P} - C_{Q}^{P}} , \quad 0 \le X_{P} \le 1.$$
 (3.14)

The dimensionless time is defined by Eq.(3.4) and the dimensionless spatial position is $X (\equiv \hat{X}/L_S)$. Figure 3.1 illustrates the geometry for the one-dimensional mass transfer problem. The PQI-function, defined by Eq.(3.2), is related to Eq.(3.12) by integrating over the solid product phase:

$$\langle \Theta^{S} \rangle (t) = \int_{0}^{1} \Theta^{S}(X, t) dX.$$
 (3.15)

At t = 0, the concentration difference functions are spatially uniform and equal to unity within their designated domain (i.e. phase). As $t \to \infty$, these functions relax to zero.

3.4 Linear Adsorption – Analytical Solution

With the pseudo-steady state assumption (see Appendix B), the difference function in the solid product phase can be represented in terms of the eigenfuctions associated with the initial boundary-value problem defined by Eqs. (B.1)-(B.4):

$$\Theta^{S}(X,t) = \sum_{n=1}^{\infty} A_{n} \cos(\lambda_{n} X) \exp(-\lambda_{n}^{2} t) , \quad 0 \le X_{S} \le 1 , \quad t > 0.$$
 (3.16)

The eigenvalues associated with the eigenfunctions (i.e., $\cos(\lambda_n X)$, n=1,2,3,...) are the roots to the following transcendental equation:

$$\lambda_{\mathbf{n}} \tan(\lambda_{\mathbf{n}}) = \alpha$$
 , $\mathbf{n} = 1, 2, 3, \dots$ (3.17)

The dimensionless group α in Eq.(3.17) compares the mass transfer resistance of the product phase with the barrier phase. This dimensionless group is a composite of the seven independent groups discussed above and is defined by

$$\frac{1}{\alpha} = \frac{\left\{\frac{L_G}{D_G} + \frac{L_P}{K_{PG}D_P} + \frac{1}{k_c}\right\}}{\left\{\frac{L_S}{K_{SG}D_S}\right\}} = \frac{\left\{\text{mass transfer resistance of the barrier phase}\right\}}{\left\{\text{mass transfer resistance of the product phase}\right\}}$$
(3.18)

Physically, $1/\alpha$ compares the series resistance to mass transfer due to the air gap, the polymer barrier, and the external surroundings to the resistance to mass transfer in the solid product phase. A package design with $\alpha >> 1$ corresponds to a situation where the mass transfer resistance of the product phase is large compared with the mass transfer resistance of the other phases. Under these conditions, the PQI-time is relatively small and, consequently, the shelf life of the blister package is relatively short. Blister packages with $\alpha < 1$ have desirable barrier characteristics. The ideal situation is to have $\alpha = 0$ (no penetration of external water), but this is not practical. Therefore, the relationship between the eigenvalues and the design parameters provides a quantitative means to identify a practical design. Table 4.3 (see Chapter 4) tabulates the first few roots to Eq.(3.17) for different values of α . The corresponding Fourier coefficients A_n in Eq.(3.16) are also given in Table 4.3.

The PQI-function can be calculated directly from Eq.(3.16) by integrating over the S-phase:

$$\langle \Theta^{S} \rangle (t) = \sum_{n=1}^{\infty} A_{n} \left[\int_{0}^{1} \cos(\lambda_{n} X) dX \right] \exp(-\lambda_{n}^{2} t) = \sum_{n=1}^{\infty} A_{n} \frac{\sin(\lambda_{n})}{\lambda_{n}} \exp(-\lambda_{n}^{2} t).$$
 (3.19)

For $t \gg 0$, the above representation is accurate with only a few terms in the series. However, for very short times, many eigenvalues must be included in the series representation. For long times, the smallest eigenvalue controls the relaxation of Eq.(3.19) with the result that

$$\underbrace{\lim_{t \to t_C}} <\Theta^S > (t) \to <\Theta^S > (t_c) \equiv <\Theta^S >_c \cong A_1 \frac{\sin(\lambda_1)}{\lambda_1} \exp(-\lambda_1^2 t_c). \tag{3.20}$$

Thus, for blister package designs that have a relatively long shelf life, the PQI-time can be calculated by using the asymptotic equation given by Eq.(3.20). Therefore,

$$t_{c} = \frac{1}{\lambda_{1}^{2}} \ln \left[\frac{A_{1} \sin(\lambda_{1}) / \lambda_{1}}{\Theta_{c}^{S}} \right] \quad (\equiv PQI-time). \tag{3.21}$$

Eq.(3.21) shows that the PQI-time depends only on the smallest root of Eq.(3.17), which provides the essential theoretical link between the PQI-time (i.e., the shelf life) and the design of the blister package.

3.6 Linear Adsorption – Numerical Solution

The unsteady-state boundary value problem defined in Section 3.5 above (also see Appendix B) can be solved numerically. For this purpose, COMSOL MULTIPHYSICS® was used. This commercial software supports the simulation of partial differential equations and boundary conditions commonly found in heat, mass, and momentum transport. It is based on a finite element method. "Mass Balance - Diffusion – Transient" analysis was the model selected under the chemical engineering module. A one dimensional flat plate of unit thickness (dimensionless) was developed. The partial differential equation, the initial conditions, and the boundary conditions were provided as user inputs. The results are summarized in Chapter 4.

3.7 Unsteady State Model for the PQI-time

Water is transported by ordinary diffusion with a constant diffusion coefficient in each phase. D_S, D_G, and D_P represent, respectively, the diffusivity of water in the S-phase, G-phase, and P-phase of the blister package (see Figure 3.1). The dimensionless

PQI-time will also be influenced by the relative sizes of the three phases: $L_P \ll L_S, L_G$. Diffusion in the polymer phase is one-dimensional and the geometry is flat. The moisture distribution is governed by the following differential equation,

$$\frac{\partial C^{P}}{\partial \hat{t}} = D_{P} \frac{\partial^{2} C^{P}}{\partial \hat{X}_{P}^{2}} , \quad 0 \le \hat{X}_{P} \le L_{P} , \quad \hat{t} > 0 .$$
 (3.22)

Diffusion in the solid product phase is also one-dimensional and the geometry is flat,

$$\frac{\partial C^{S}}{\partial \hat{t}} = D_{S} \frac{\partial^{2} C^{S}}{\partial \hat{x}_{S}^{2}} , \quad 0 \le \hat{x}_{S} \le L_{S} , \quad \hat{t} > 0 .$$
 (3.23)

The geometry of the air gap is complicated. In general, the concentration of water in the G-phase is governed by 3D unsteady-state diffusion:

$$\frac{\partial C^{G}}{\partial \hat{\mathbf{t}}} = D^{G} \hat{\nabla}^{2} C^{G} . \tag{3.24}$$

Application of the divergence theorem and the condition that the water flux is continuous across an interface gives (Kim, 1998)

$$V_{G} \frac{d < C >^{G}}{d \hat{t}} = S_{GP} D_{P} \frac{\partial C^{P}}{\partial \hat{X}_{P}} \bigg|_{\hat{X}_{P} = 0} - S_{SG} D_{G} \frac{\partial C^{G}}{\partial \hat{X}_{S}} \bigg|_{\hat{X}_{S} = 1}, \quad \hat{t} > 0.$$
(3.25)

The above equation assumes that the flux is spatially uniform over the 2D interface. S_{SG} represents the total interfacial area (both sides of the symmetrical tablet) available for mass transfer between the S-phase and the G-phase (air gap); S_{GP} represents the interfacial area available for mass transfer between the G-phase (air gap) and the P-phase. The parameter S_{BG} represents the interfacial area between the backing and the G-phase.

This area does not appear in the above equation because the moisture flux across the backing is zero. If the concentration of water on the gas side near the interface equals the spatial average concentration of water in the G-phase (i.e., well-mixed assumption, $D_G \square D_S, D_P$), then

$$C^{S}(L_{S},\hat{t}) = K_{SG} < C^{G} > (\hat{t})$$
 (3.26)

$$C^{P}(0,\hat{t}) = K_{PG} < C^{G} > (\hat{t})$$
 (3.27)

The continuity of flux across the two internal interfaces has already been incorporated into the macroscopic equation for the G-phase given above (see Eq.(3.25)). The water in the S-phase near the SG-interface is assumed to be in thermodynamic equilibrium with the water in the G-phase near the SG-interface (see Figure 3.1). The local thermodynamic equilibrium assumption (see Bird et al., 2002; Rice and Do, 1995; Smith and Peppas, 1991; Kim et al., 1998) is also imposed on the PG- and GP-interfaces. At steady state, thermodynamic equilibrium applies everywhere and the water concentration is spatially uniform in each phase. The temperature-dependent, thermodynamic distribution coefficients at the SG-interface and the PG-interface are denoted as K_{SG} and K_{PG}. Thermodynamic equilibrium and continuity of flux across the polymer/environmental interface implies that

$$C^{P}(L_{P},\hat{t}) = K_{PG}C^{E}(\hat{X}_{E} = 0,\hat{t})$$
 (3.28)

$$D_{\mathbf{p}} \frac{\partial C^{\mathbf{p}}}{\partial \hat{X}_{\mathbf{p}}} \bigg|_{\hat{X}_{\mathbf{p}} = L_{\mathbf{p}}} = D_{\mathbf{E}} \frac{\partial C^{\mathbf{E}}}{\partial \hat{X}_{\mathbf{E}}} \bigg|_{\hat{X}_{\mathbf{E}} = 0 \ (\hat{X}_{\mathbf{p}} = L_{\mathbf{p}})}$$
(3.29)

The flux in the surrounding gas (or environmental) phase (E-phase) is determined by introducing a convective mass transfer coefficient:

$$-D_{E} \frac{\partial C^{E}}{\partial \hat{X}_{E}} \Big|_{\hat{X}_{E}=0 \ (\hat{X}_{P}=L^{P})} = k_{c} \left[C^{E}(0,\hat{t}) - C_{\infty}^{E} \right]$$
(3.30)

The following condition for disk geometry assumes that the water concentration in the air gap is spatially uniform.

$$\frac{\partial C^{S}}{\partial \hat{X}_{S}} \Big|_{\hat{X}_{S}=0} = 0 \quad \text{(disk --- symmetry)}$$
 (3.31)

Making the above equations dimensionless introduces four dimensionless groups

$$N_{\tau}^{2} = \frac{L_{P}^{2} / D_{P}}{L_{S}^{2} / D_{S}}$$
 (3.32)

$$N_{S} = \frac{V_{S}K_{SG}}{V_{G}} \tag{3.33}$$

$$N_{P} = \frac{V_{P}K_{PG}}{V_{G}} \tag{3.34}$$

 N_{τ}^2 compares the characteristic diffusion time of the P-phase with the characteristic diffusion time of the S-phase. The Biot number for interfacial mass transfer, defined as

$$Bi = \frac{k_c L_P}{D_P} \qquad , \tag{3.35}$$

also influences the PQI-time. Previous studies usually assume that $Bi\to\infty$. Although this assumption yields the simplification that the water at the PG-interface is instantaneously at its final steady state condition, the analysis developed hereinafter retains the possibility that the external resistance to mass transfer may limit the rate of absorption.

In summary, the dimensionless PQI-time introduced by Eq. (3.7) above depends on the foregoing dimensionless groups and the critical PQI coefficient, Θ_c^S . Thus,

$$t_{c} = F(N_{S}, N_{P}, N_{\tau}, Bi, \Theta_{c}^{S})$$
(3.36)

Figure 3.1 illustrates the geometry for the one-dimensional mass transfer problem. The PQI-function, defined by Eq.(3.2), is related to Eq.(3.12) by integrating over the solid product phase:

$$\langle \Theta \rangle^{S}(t) \equiv \int_{0}^{1} \Theta^{S}(X_{S}, t) dX_{S}.$$
 (3.37)

At t = 0, the concentration difference functions are spatially uniform and equal to unity within their designated domain (i.e. phase). As $t \to \infty$, these functions relax to zero. As indicated in Appendix C, the difference function in the solid product phase can be represented in terms of eigenfunctions associated with the initial boundary-value problem defined by Eqs. (C.1)-(C.4):

$$\begin{pmatrix} \Theta^{S} \\ \Theta^{P} \end{pmatrix} = \sum_{n=1}^{\infty} A_{n} \begin{pmatrix} F_{n}^{S} \\ F_{n}^{P} \end{pmatrix} \exp(-\lambda_{n}^{2}t) , \quad t > 0$$
(3.38)

$$F_{n}^{S}(X_{S}) = B_{1n}^{S} \sin(\lambda_{n} X_{S}) + B_{2n}^{S} \cos(\lambda_{n} X_{S})$$
(3.39)

$$F_{n}^{P}(X_{P}) = B_{1n}^{P} \sin(N_{\tau}\lambda_{n}X_{P}) + B_{2n}^{P} \cos(N_{\tau}\lambda_{n}X_{P})$$
(3.40)

The eigenvalues associated with the eigenfunctions are the roots to the following transcendental equation:

$$\Im(\lambda_n) = \lambda_n + N_S \tan(\lambda_n) + \frac{N_P}{N_\tau} \frac{(N_\tau \lambda_n \tan(N_\tau \lambda_n) - Bi)}{(N_\tau \lambda_n + Bi \tan(N_\tau \lambda_n))} = 0$$
 (3.41)

3.8 GAB Adsorption - Numerical Solution

The use of a GAB-isotherm (see Eq.(2.6) above) at the product/air-gap interface makes the boundary value problem non-linear. The presence of this non-linearity warrants the use of a numerical method. A finite element solver supported by COMSOL MULTIPHYSICS® was used to develop numerical solutions to the boundary value problem. See Appendix D for the set up and Chapter 4 for the results.

3.9 PSSA Model with a GAB Isotherm – Experimental Validation

The pseudo-steady state model was validated by comparing the predicted results with the experimental results reported by Allen (1994). Allen conducted sorption experiments on 20 mg Deltasone® tablets at room temperature (25°C) exposed to humid air with a relative humidity varying from 0 to 92%. Fourteen sorption experiments were conducted on the product tablets. The diffusion coefficients and the GAB-coefficients were determined from this data. The diffusion coefficients reported in Allen's thesis were confirmed as part of this study (see Section 2.4 and Appendix E). The diffusion coefficients are functions of the temperature and the local moisture concentration. Allen used an average diffusion coefficient to analyze the shelf life of blister packages based on a finite difference model developed by Kim (1992).

The polymer used for the studies was a laminate of PVC and ACLAR®. Allen delaminated the polymer composite to obtain separate films for direct testing. Both polymer films were individually studied for moisture uptake. The data obtained were used to determine the diffusion coefficients of the polymer films. Allen estimated an effective diffusion coefficient of the polymer laminate barrier based on the following expression:

$$\frac{L_{PVC}}{D_{PVC}} + \frac{L_{ACLAR}}{D_{ACLAR}} = \frac{L_{P}}{D_{P}}.$$
(3.42)

In the above equation, Dp represents the diffusion coefficient of the composite polymer barrier; Lp is the thickness of the polymer barrier; LpVC and Laclar represent, respectively, the thickness of the PVC and the ACLAR® films; and, DpVC and Daclar represent the diffusion coefficients of the two individual polymer films. The thermodynamic moisture distribution coefficients (i.e., Henry's law constant for linear adsorption isotherms) for the polymer/environment interface were also determined from the moisture sorption data. A confirmation of diffusion coefficients reported by Allen for the polymer phase was carried out in the same fashion as the confirmation for the tablets (see Section 2.5 above).

The moisture sorption data obtained from the pseudo-steady state model with the GAB-isotherm was compared with the experimental data reported by Allen (1994). The parameters used in the model to generate the moisture sorption results were also selected from Allen's work. The data used in the comparison were for samples tested at a relative humidity of 80% and a relative humidity of 90%. Table 4.1 summarizes the thermodynamic and transport properties reported by Allen(1994). These parameters were used as the "base" case for the parametric study presented in Chapter 4.

CHAPTER 4

PARAMETRIC STUDIES OF THE PSEUDO-STEADY STATE ABSORPTION (PSSA-) MODEL

4.1 Introduction

The pseudo-steady state absorption (PSSA) model can be used with linear and non-linear sorption isotherms. The effect of the various environmental and physical parameters on the sorption of moisture through the blister packaged pharmaceutical product at various storage conditions is discussed in the following sections.

4.2 Input Data for the PSSA Model

The moisture sorption isotherms at 25°C for the tablet and for the polymer barrier were previously determined by Allen (1994) as summarized in Chapter 3 above. The physical and environmental parameters used in the PSSA model are listed in Table 4.1 below.

4.3 PSSA Model --- Linear Isotherm

The pseudo-steady state absorption model with linear isotherms is defined in Sections 3.3 and 3.4 above as well as in Appendix A and Appendix B. Table 4.2 shows the range over which each of the dimensionless groups governing the linear PSSA model was varied. Table 4.3 gives the first three eigenvalues and Fourier coefficients for resistance ratios in the range: $0.1 \le \alpha \le 0.5$. The results show that the eigenvalues are well separated, which partially justifies the use of Eq.(3.21) for the shelf life estimate.

Table 4.1 Base Case Parameters for Component Phases (Allen, 1994)				
Component Phase	Symbol	Values		
External Environment	Т	25 ℃		
	$ m A_W imes 100\%$, % relative humidity	80%, 90%		
Polymer Composite Barrier (PVC and ACLAR®)	Dp (average)	$2 \times 10^{-9} \text{ cm}^2/\text{s}$		
	Lp (full thickness)	0.0023 cm		
	$K_{PG} = K_{GP}$ (composite)	$\frac{(g \text{ H}_2\text{O})/(\text{cm}^3 \text{ polymer})}{(g \text{ H}_2\text{O})/(\text{cm}^3 \text{ air})}$		
	V _P , total volume	30 mm ³		
	$D_{\mathbf{S}}$	$0.996 \times 10^{-6} \text{ cm}^2/\text{s}$		
Deltasone® Tablet	L _S (half thickness)	0.196 cm		
	GAB parameters (a ₃ , a ₂ , a ₁)	(-1.79,+1.92, +0.064)		
	$\kappa_{ ext{SG}}$	$\frac{1}{a_1} = 16 \frac{(g \text{ H}_2\text{O})/(\text{cm}^3 \text{ product})}{(g \text{ H}_2\text{O})/(\text{cm}^3 \text{ air})}$		
	V _S , volume	308 mm ³		
Air Gap	V_G , volume	492 mm ³ , $L_G = 0.02$, mm		

Table 4.2 Scope of Parametric Study for the Linear PSSA Model $L_S\cong 0.196\,\text{cm}\,(\text{half thickness})\;,\;D_S\cong 10^{-6},\text{cm}^2\,/\,\text{s}\;,\;L_S^2\,/\,D_S\cong 11\;\text{hours}$

PSSA-Parameter	Base (Table 4.1)	Scope	Reference
$\Theta_{\mathbf{c}}^{\mathbf{S}}$	0.5	$0 < \Theta_{\mathbf{c}}^{\mathbf{S}} < 1$	Figure 4.1
$N_1 \equiv L_G / L_S$	0.6	N ₁ << 1	Figure 4.1
$N_2 \equiv L_P / L_S$	0.1	$0.001 \le N_2 \le 0.1$	Figure 4.1
$N_3 \equiv D_G / D_S$	8	N ₃ = ∞	-
$N_4 \equiv D_P / D_S$	0.002	$0.0001 \le N_4 \le 1$	Figure 4.1
$Bi = N_5 = k_c L_P / D_P$	8	N ₅ = ∞	-
$N_6 = K_{SG}$	16	$N_6 = 16$	-
$N_7 \equiv K_{PG}$	125	N ₇ = 125	-
N7/N6	7.8	$N_7/N_6 = 7.8$	-
$\alpha \cong \frac{L_S}{L_P} \frac{K_{PG}}{K_{SG}} \frac{D_P}{D_S} = \frac{1}{N_2} \frac{N_7}{N_6} N_4$ (see Eq.(3.18))	0.15	0.001 ≤ α ≤ 100	Figure 4.1 Figure 4.2 Table 4.3 Table 4.4

Т	Table 4.3: Eigenvalues and Fourier Coefficients for the Linear PSSA-Model				
$\lambda_n \tan(\lambda_n) = \alpha$		$_{\mathbf{n}})=\alpha$	$A_{n} = \frac{\int_{0}^{1} \cos(\lambda_{n}X)dX}{\int_{0}^{1} \cos^{2}(\lambda_{n}X)dX}$		
α	n	$\lambda_{\mathbf{n}}$	A _n		
0.1	1	0.31106	+ 1.0161		
	2	3.1731	- 0.019661		
	3	6.2991	+ 0.0050275		
0.2	1	0.43285	+ 1.0311		
	2	3.2039	- 0.038153		
	3	6.3148	+ 0.009977		
0.3	1	0.5218	+ 1.045		
	2	3.2341	- 0.05554		
	3	6.3305	+ 0.014844		
0.4	1	0.59325	+ 1.058		
	2	3.2636	- 0.071899		
	3	6.3461	+ 0.019633		
0.5	1	0.65328	+ 1.0701		
	2	3.2923	- 0.087281		
	3	6.3616	+ 0.024338		

Figure 4.1 illustrates the temporal relaxation of the PQI-function for different values of the resistance ratio α . The graph is generated by using Eq.(??.21). For a blister package with $\alpha=0.1$, Figure 4.2 shows that for $<\Theta>^S\cong 0.5$, the dimensionless time $t\approx 8$. Therefore, if the PQI coefficient $\Theta_c^S=0.5$ and if $L_S^2/D_S=11$ hours (see Table 1), then the shelf life predicted by the pseudo-steady state model is about 3.5 days. For a fixed value of Θ_c^S , the shelf life clearly increases as α decreases.

Figure 4.2 illustrates the variation of the PQI-time with α . As expected, the PQI-time increases as the resistance ratio α decreases for a fixed value of Θ_c^S (= 0.5). In the "barrier" regime (α < 1), small changes in blister design can have a significant influence on the shelf life of the product. On the other hand, for α > 1, "large" changes in the blister design have little effect on the shelf life.

4.4 PSSA Model (GAB Isotherm)

Figure 4.3 and 4.4 compare the experimental packaged tablet moisture content curves (Allen, 1994) with the curves generated by the PSSA-model (GAB isotherm) using COMSOL MULTIPHYSICS® for different values of α at relative humidities of 80 & 90%. This result shows a marked difference in the sorption data between the pseudo steady state model and the experiments. One variable which was not accounted for was the diffusion coefficient of the laminated polymer in the formed blister, which may have

Table 4.4: Eigenvalues and Fourier Coefficients for Linear Conjugate Absorption (see Appendix C)

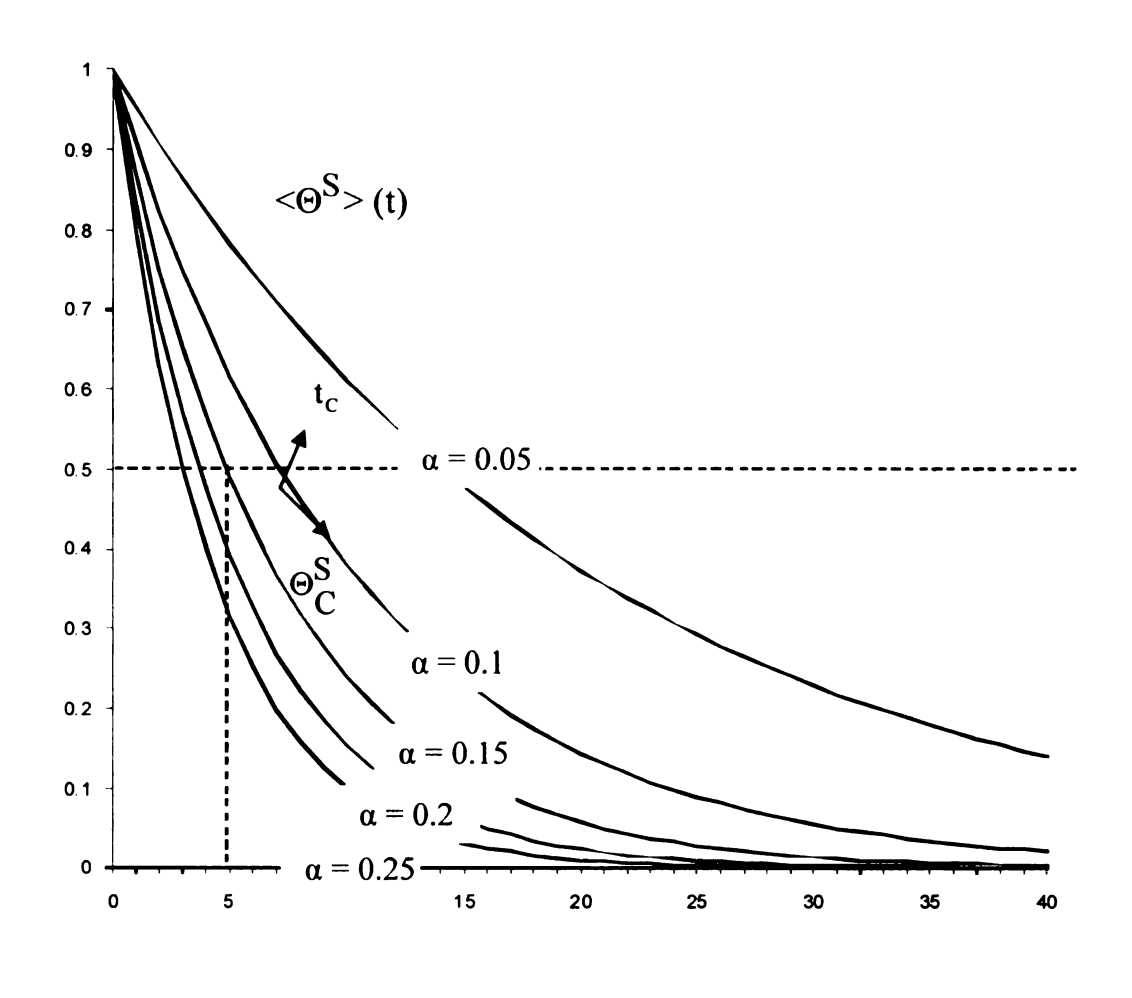


Figure 4.1 The Effect of α on the Volume Average Moisture Concentration of the Drug for the Linear PSSA-Model.

t

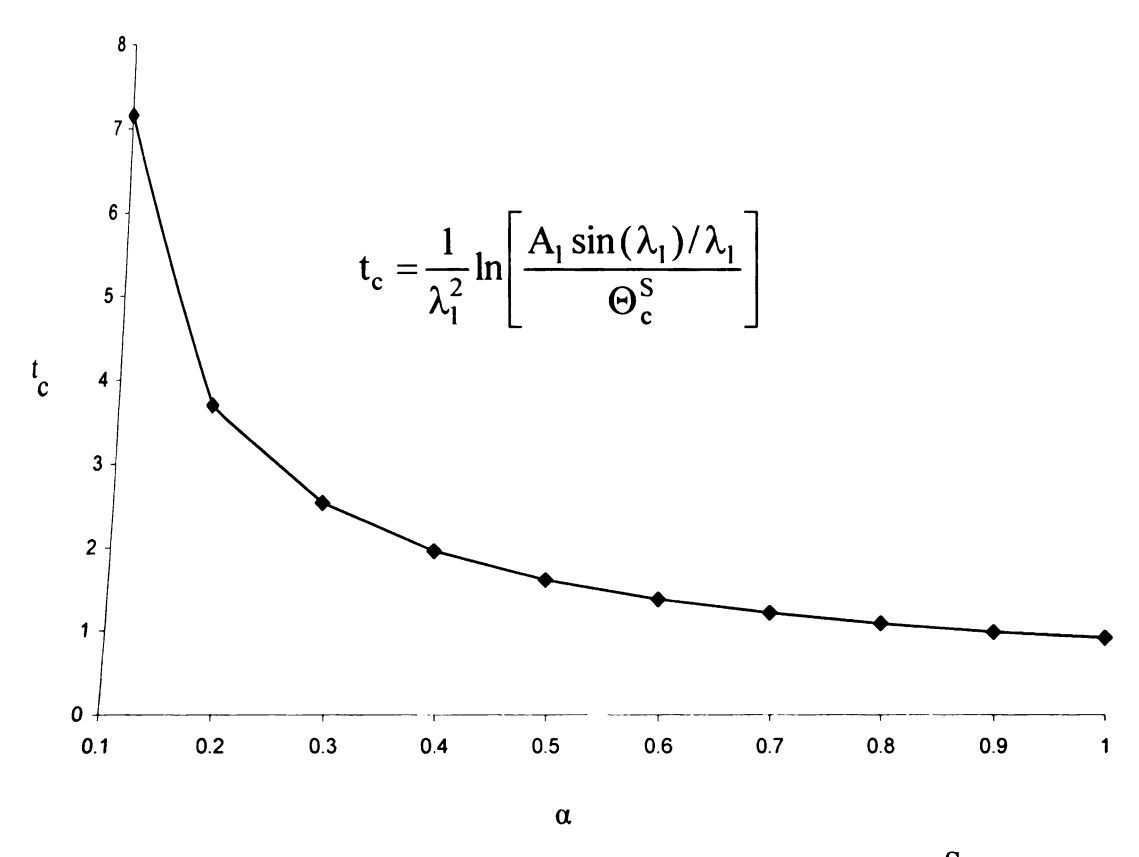
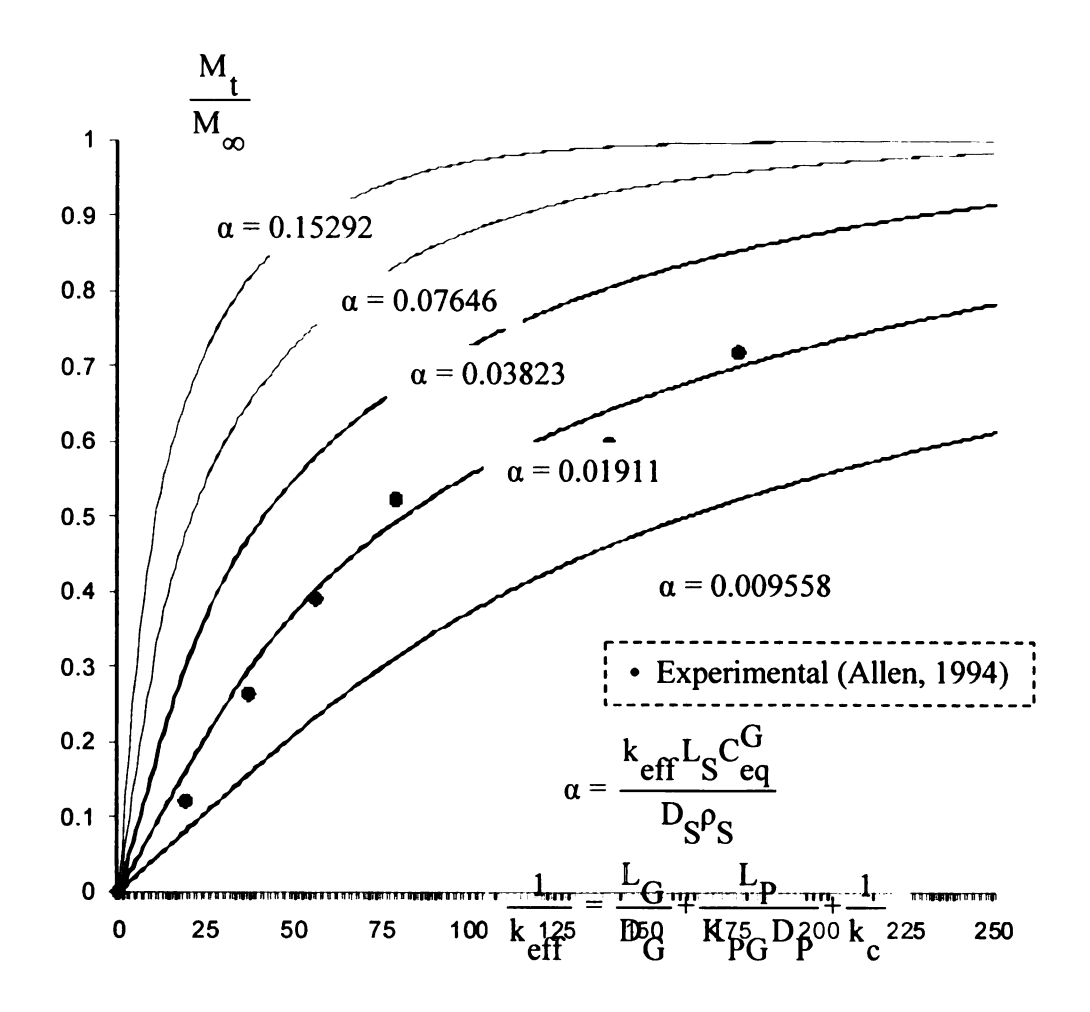


Figure 4.2 The Effect of α on the Shelf Life for the Linear PSSA-Model (Θ_c^S = 0.5).



$$t = \frac{\hat{t}D_S}{L_S^2}$$

Figure 4.3 Comparison of Experimental Results with the Nonlinear PSSA-Model (GAB Isotherm) for $A_{w} = 0.80$ (see Appendix D for the experimental parameters).

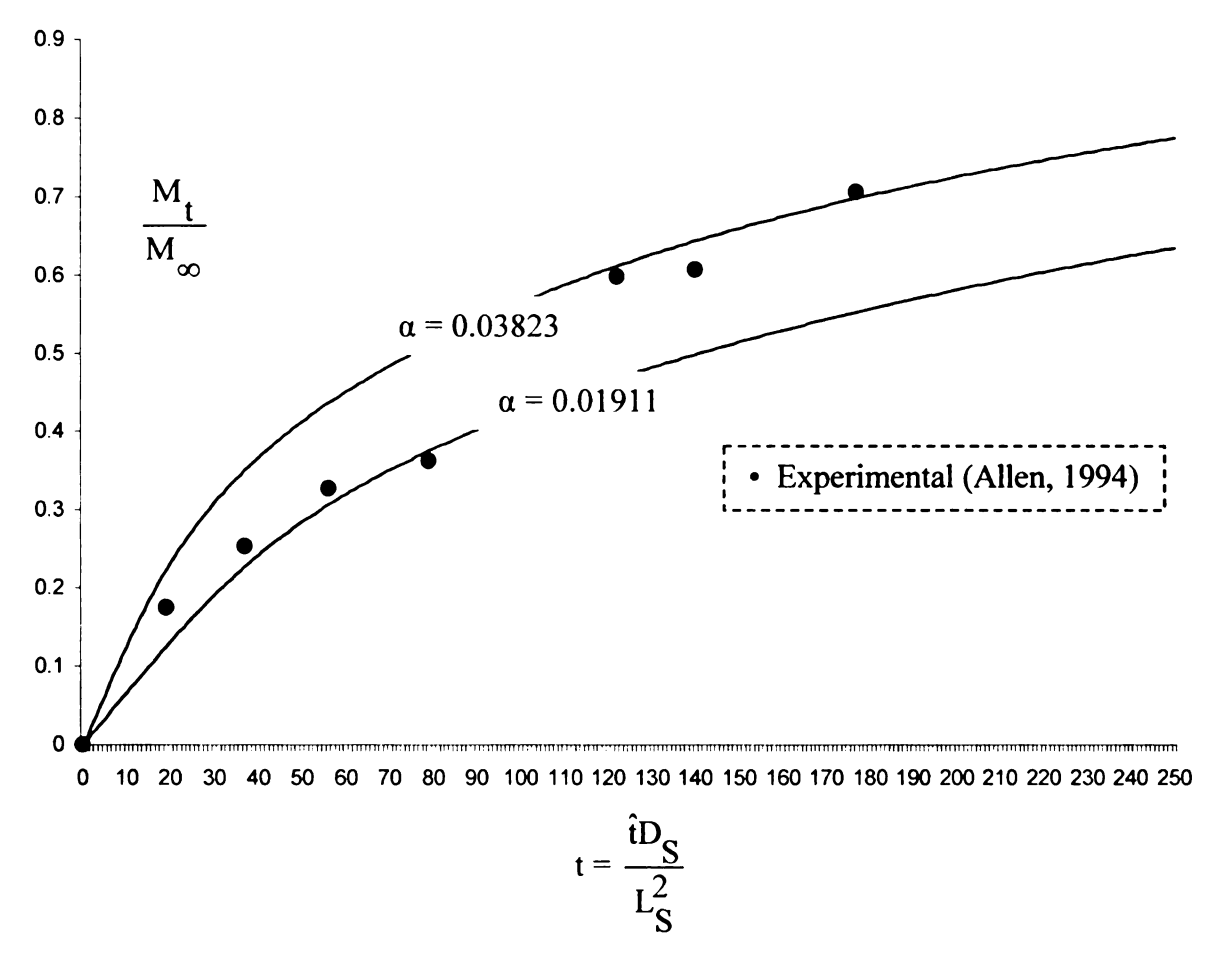


Figure 4.4 Comparison of Experimental Results with the Nonlinear PSSA-Model (GAB Isotherm) for $A_{\mathbf{W}} = 0.90$ (see Appendix D for the experimental parameters).

undergone structural changes during the forming process itself on account of the heat and stress involved. A more detailed comparison of the experimental and the calculated results was undertaken with the diffusion coefficient of the package as a variable. This result is also illustrated in the figures. As seen from the results, the experimental results imply that for $\alpha = 0.019$.

Figure 4.5 shows the experimental sorption of moisture in the tablet, the PVC, ACLAR® and the blister package containing the tablet at 80% RH. On close evaluation of the moisture sorption data for the tablet, the polymer and the blister packaged tablet; we can see a clear anomaly in the time required by the moisture to reach its equilibrium concentration. The difference is all the more magnified for the particular example chosen. The time required for the moisture in the blister packaged tablet to reach its equilibrium value is around 10,000 hours while the tablet, PVC and the ACLAR reach equilibrium in 10, 4 and 2 hours respectively. This result prompts a question as to why when the two entities i.e. the tablet and the polymer which both have an equilibrium time of nearly a day each are put together to form a package the equilibrium time for the moisture in the blister packaged tablet increases to almost one year. When the two systems in question are compared the only additional factor in the blister packaged tablet is the presence of an air gap between the polymer and the tablet phase. Does the air gap phase cause this difference? Examination of the diffusion coefficients in the three phases says otherwise. The diffusion coefficient in the air gap phase is very negligible compared to the polymer and the product phases which is a direct validation of our initial assumption that the moisture concentration in the air gap phase is not variable and can be assumed as

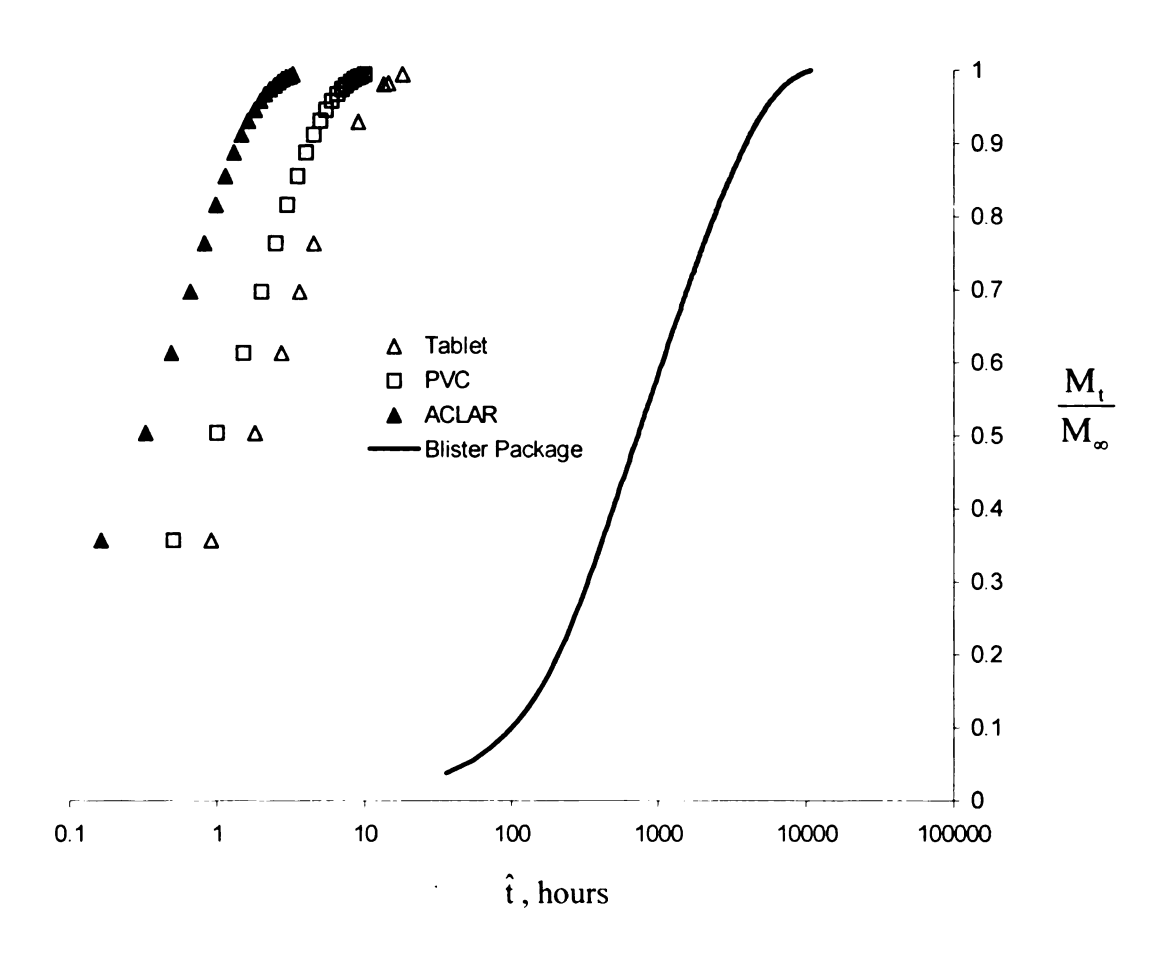


Figure 4.5 Moisture Absorption by Individual Constituents of a Blister Package (nonlinear PSSA-model $A_W = 0.80$).

spatially uniform. This result still does not rule out the influence of the air gap phase. Hence, a detailed study of the moisture distribution in the air gap phase was warranted.

Figure 4.6 explains this anomaly by studying the variation of the flux at the tablet air gap interface with time in the blister packaged tablet. We can see that the flux increases rapidly initially and then slowly approaches its equilibrium value i.e. zero flux, which essentially means no more moisture diffusing into the package. Since the diffusive flux decreases exponentially over a long duration of time, the moisture inside the blister packaged tablet takes a long time to reach equilibrium. The results give us a better understanding of the role of the air gap phase in protecting the product from moisture ingress. It takes a long amount of time for the moisture concentration to build up in the air gap phase even though the diffusion coefficient for the air gap phase is very high; the air gap phase essentially acts as a time barrier for the moisture

Figure 4.7 illustrates the variation of moisture sorption in the blister packaged tablet as a function of the relative humidity of the storage environment. As expected, the moisture sorption increases with an increase in the environmental RH.

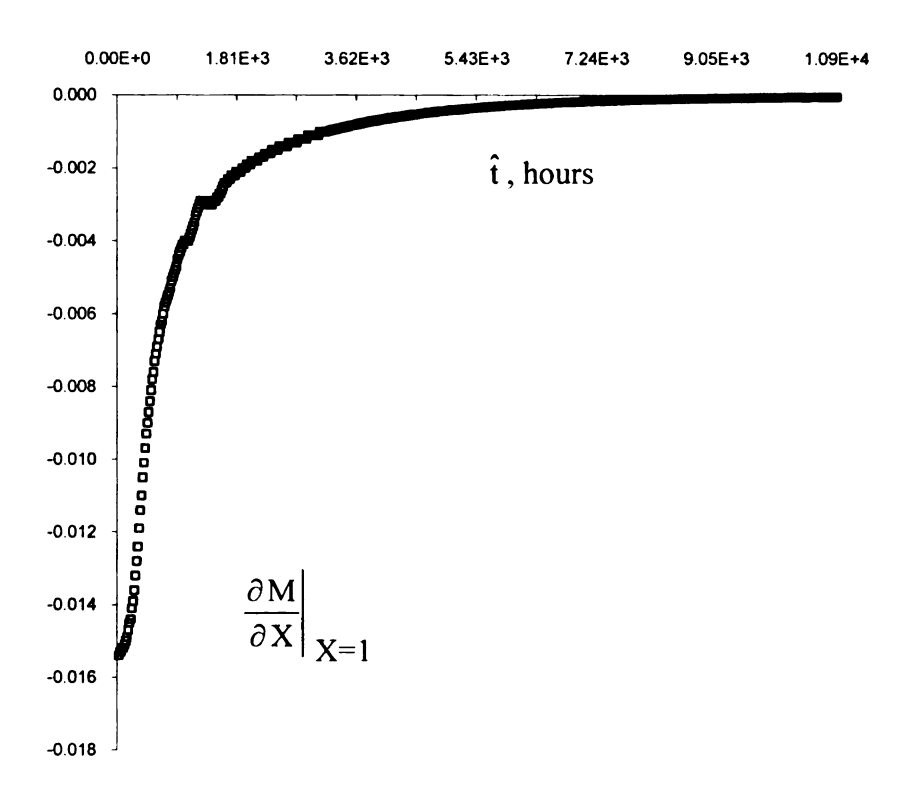


Figure 4.6 Transient Moisture Flux at the Product/Air Gap Interface in a Blister Package for $A_W = 0.80$ (nonlinear PSSA-Model).

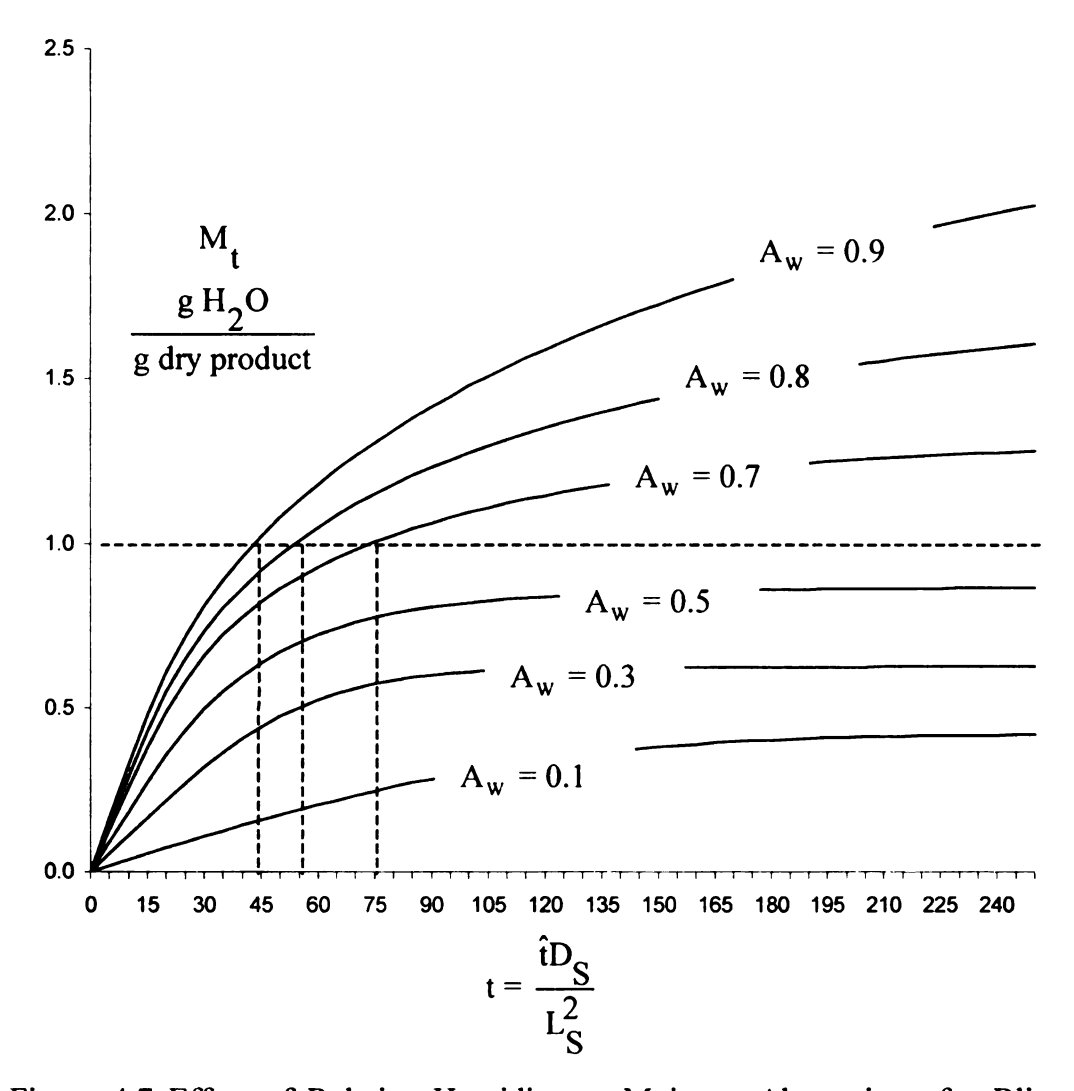


Figure 4.7 Effect of Relative Humidity on Moisture Absorption of a Blister Package Based on the Non-linear PSSA-Model ($L_S^2/D_S^2=11$ hours, $\alpha=0.01911$).

CHAPTER 5 CONCLUSIONS

Diffusion coefficient of the packaging polymer is a very important property and has to be determined accurately especially for multi-laminates. Figure 4.3 shows that the PSSA (GAB isotherm) sorption curve agrees with experimental data (Allen, 1994) for $\alpha = 0.01911$, which corresponds to a polymer diffusion coefficient of $D_P = 5 \times 10^{-10} \text{cm}^2/\text{s}$. But, Allen used a diffusion coefficient for the polymer laminate of $D_P = 2 \times 10^{-9} \text{cm}^2/\text{s}$ ($\alpha = 0.03822$). The diffusion coefficient of the laminate was calculated based on the thickness and the individual diffusion coefficients of moisture in PVC and ACLAR films (Crank, 1956) similar to heat transfer through a multi-layered wall. The effect of the adhesive layer on the diffusion coefficient of the polymer laminate was not taken into account. This is the reason, the experimental data did not agree with the moisture sorption calculations from her model.

GAB moisture sorption isotherm parameters for the product which has to be packaged also determines the ease with which the shelf life time can be assessed for the system. Certain levels of the environment humidity allow the linearization of the isotherm with negligible errors which in turn guarantees an analytical solution. An analytical solution saves us time and resources involved in numerical computations. Figure 2.2 depicts the GAB isotherm and the corresponding linear isotherm for GAB parameters, $a_3 = -1.79$, $a_2 = 1.922$, $a_1 = 0.064$. The linear isotherm for the particular case chosen always predicts a high value of M corresponding to the storage humidity (A_W). Hence, the linear isotherm will always predict a PQI-time which is way lower than the actual PQI-time because of the presence of a higher amount of driving force (M).

Therefore, the linear isotherm is not a good approximation to the GAB isotherm for the chosen example system.

The time taken for the moisture in a blister packaged product to attain equilibrium when in storage is of the order of several months to years depending on the product, the packaging system and the storage conditions. The time taken for the moisture in just the packaging polymer or in the product alone as a single entity to attain equilibrium is just a matter or hours or a day (Figure 4.6). This anomaly prompts a question as to whether the introduction of such a small air gap can increase the equilibrium time to the extent as shown. The variation of the diffusive flux at the product air gap interface was studied (Figure 4.7). The diffusive flux is very high initially but reduces exponentially to zero as time increases, thereby reducing the amount of moisture diffusing into the tablet. This property of the diffusive flux is what prolongs the shelf life of the pharmaceutical product

Pseudo steady state assumption has been shown to be a valid approach to solve the boundary value problem analytically. The rigorous analysis of the same is discussed in section 3.6 (Appendix C & Appendix F).

Long time analysis of the pseudo steady state problem with linear moisture sorption isotherms yields a simple analytic expression for the shelf life time of the product (Eq.(3.21)). This can be used as a simple tool for pre-testing a system before the actual stability testing for a package is done.

PSSA-model comports very well with an earlier comprehensive experimental study of moisture uptake by 20 mg Deltasone® tablets in blister packages (see Allen, MS Thesis, The School of Packaging, Michigan State University, 1994). Figure 4.3 shows that the moisture sorption curves generated by the PSSA model with GAB isotherms agrees well with the experimental data at 80% RH for a value of $\alpha = 0.01911$. For this case, the parameter α depends explicitly on the physical and geometrical properties of the PVC/ACLAR moisture barrier as well as the external mass transfer coefficient for a stagnant humid air film. Thus, the PSSA-model provides a means to benchmark the shelf life of a class of blister packages as well as a means to interpret the results of specific testing protocols. The PSSA-model has been validated using the experimental data (Allen, 1994).

CHAPTER 6 RECOMMENDATIONS

The effect of pill geometry on the moisture distribution can be studied. A model analogous to the one developed in the present study which employs the pseudo steady state condition can be formulated for various geometries like cylinders, spheres etc. The initial boundary-value problem defined by Appendix A can be formulated as an axisymmetric problem and as a spherically symmetric problem. A complementary model that assumes a pseudo-state approximation for the S-phase and an explicit unsteady state model for the P-phase can be developed. The problem can be designed to analyze the impact of curvature on the PQI-time.

The PSSA-model can be used as the basis for developing shelf life design criteria for blister packages. The design criteria could be used to design a minimum set of experiments which have to be carried out to generate sufficient moisture distribution data (short time analysis), which can be used to determine the different variables in the blister system i.e. the diffusion coefficients of the individual phases etc.

Shelf life models for products which can be influenced by the other constituents of the air like nitrogen, oxygen etc. in addition to moisture can be determined by using the principles of mass transport, those involving multi-component diffusion.

APPENDICES

APPENDIX A. One-Dimensional Diffusion for Linear Adsorption Isotherms

The objective of this appendix is to define the initial boundary-value problem for one-dimensional absorption in a blister package. The moisture adsorption isotherms at the phase interfaces are assumed to be linear. Appendix A supports the discussion in Chapter 3 as well as Appendices B and C below. The following dimensionless variables are used to characterize the moisture concentration in each phase (see Figure 3.1):

$$\Theta^{S}(X,t) = \frac{C_{eq}^{S} - C^{S}(X,t)}{C_{eq}^{S} - C_{o}^{S}}$$
(A.1)

$$\Theta^{G}(X,t) = \frac{C_{eq}^{G} - C^{G}(X,t)}{C_{eq}^{G} - C_{o}^{G}}$$
(A.2)

$$\Theta^{P}(X,t) = \frac{C_{eq}^{P} - C_{o}^{P}(X,t)}{C_{eq}^{P} - C_{o}^{P}}$$
(A.3)

The above dimensionless concentration difference functions satisfy the following initial boundary value problem.

Differential Equations

$$\frac{\partial \Theta^{S}}{\partial t} = \frac{\partial^{2} \Theta^{S}}{\partial X^{2}} , \quad 0 \le X \le X_{S} \equiv 1 , \quad t > 0$$
 (S-phase) (A.4)

$$\frac{\partial \Theta^{G}}{\partial t} = N_{3} \frac{\partial^{2} \Theta^{G}}{\partial x^{2}} , \quad 0 \le X \le X_{G} \equiv 1 , \quad t > 0 \quad (G - phase)$$
 (A.5)

$$\frac{\partial \Theta^{P}}{\partial t} = N_4 \frac{\partial^2 \Theta^{P}}{\partial X^2} , \quad 0 \le X \le X_P \equiv 1 , \quad t > 0 \quad (P - phase)$$
 (A.6)

Initial Conditions

The definitions of the dimensionless concentration differences imply that

$$\Theta^{\mathbf{S}}(\mathbf{X},0) \equiv 1 \quad , \quad 0 \le \mathbf{X} \le 1 \tag{A.7}$$

$$\Theta^{G}(X,0) = 1$$
 , $0 \le X \le 1$ (A.8)

$$\Theta^{\mathbf{P}}(X,0) = 1$$
 , $0 \le X \le 1$ (A.9)

Boundary Condition at the Center of the Product Phase

The assumption that the moisture distribution in the product phase is symmetric about the plane of symmetry (see Figure 3.1) implies that

$$\frac{\partial \Theta^{S}}{\partial X}\bigg|_{X=0} = 0 \quad , \quad t > 0 \, . \tag{A.10}$$

Equilibrium and Continuity of Flux on Internal Interfaces

Thermodynamic equilibrium and continuity of water flux across the SG-interface at $X_S = 1$ and the GP-interface at $X_G = 1$ require the following four conditions:

$$\Theta^{S}\Big|_{X_{S}=1} = \Theta^{G}\Big|_{X_{S}=1}$$
, $t > 0$ (SG-interface); (A.11)

$$\frac{\partial \Theta^{S}}{\partial X} \bigg|_{X_{S}=1} = \frac{N_{3}}{N_{6}} \frac{\partial \Theta^{G}}{\partial X} \bigg|_{X_{S}=1}, \quad t > 0 \quad (SG-interface);$$
(A.12)

$$\Theta^{G}\Big|_{X_{G}=1} = \Theta^{P}\Big|_{X_{G}=1}$$
, $t > 0$ (GP-interface); and, (A.13)

$$\frac{\partial \Theta^{G}}{\partial X} \bigg|_{X_{G}=1} = \frac{N_{4}N_{7}}{N_{3}} \frac{\partial \Theta^{P}}{\partial X} \bigg|_{X_{G}=1}, \quad t > 0 \quad (GP-interface). \tag{A.14}$$

Boundary Condition at the PG-Interface

The idea of thermodynamic equilibrium and continuity of water flux across the PGinterface at $X_P = 1$ implies that

$$\frac{\partial \Theta^{P}}{\partial X} \bigg|_{X_{P}=1} = -\frac{N_{5}}{N_{2}N_{7}} \Theta^{P} \bigg|_{X_{P}=1} , \quad t > 0 \quad (PG-interface).$$
 (A.15)

In Eq.(A.15), a Biot number (i.e., N_5) is introduced at the PG-interface to account for convective mass transfer. If $N_5 = N_2N_7$, then $\Theta^P \square 0$ at $X_P = 1$. Physically, this means that the PG-interface is in thermodynamic equilibrium with the humid air far from the PG-interface surrounding the blister package (i.e., no external resistance to mass transfer).

The characteristic length and time scales used in the above formulation are defined as follows

$$X = \frac{\hat{X}}{L_S} \qquad t = \frac{\hat{t} D_S}{L_S^2}. \tag{A.16}$$

The geometric ratios are defined as $N_1 \equiv L_G/L_S$ and $N_2 \equiv L_P/L_S$, where L_S is the half width of the symmetric drug tablet (see Figure 3.1). The diffusivity ratios are defined as $N_3 \equiv D_G/D_S$ and $N_4 \equiv D_P/D_S$; and, the Biot number is

$$N_5 \equiv \frac{k_c L_P}{D_P} . \tag{A.17}$$

The thermodynamic distribution coefficients at the SG-interface and the PG-interface are $N_6 = K_{SG}$ and $N_7 = K_{PG}$ (linear adsorption isotherms). Desorption of moisture from the polymer barrier at the GP-interface (see Figure 3.1) is assumed to follow the same isotherm as the PG-interface (no hysteresis). For a composite polymer barrier, the

adsorption isotherm would be a property of the outer laminate and the desorption isotherm would be a property of the inner laminate. For this situation $(PVC/ACLAR@),\ K_{GP}\neq K_{PG}\ .$ The parametric study in Chapter 4 assumes that $K_{GP}=K_{PG}\ .$

APPENDIX B. Pseudo-Steady State Absorption Model

An approximate solution to the initial boundary-value problem defined in Appendix A can be developed by assuming that the moisture concentration across the thin polymer barrier and the air gap rapidly adjusts to the relatively slow unsteady absorption process associated with diffusion into the solid product phase. Thermodynamic equilibrium and continuity of water flux across each interface, together with the idea that the moisture flux is quasi-steady across the polymer barrier and the air gap, yields the following initial boundary value problem for the concentration difference function within the solid product phase (Bird et al., 2002):

Differential Equation

$$\frac{\partial \Theta^{S}}{\partial t} = \frac{\partial^{2} \Theta^{S}}{\partial x^{2}} \quad , \quad 0 \le X \le 1 \quad , \quad t > 0$$
 (B.1)

Initial Condition

$$\Theta^{\mathbf{S}}(\mathbf{X},0) \equiv 1 \quad , \quad 0 \le \mathbf{X} \le 1 \tag{B.2}$$

Boundary Condition at the Center of the Product Phase

$$\frac{\partial \Theta^{S}}{\partial X}\bigg|_{X=0} = 0 \quad , \quad t > 0 \, . \tag{B.3}$$

Boundary Condition at the SG-Interface

The pseudo-steady state approximation applied to the air gap and the polymer barrier yields the following boundary condition at the SG-interface:

$$\frac{\partial \Theta^{S}}{\partial X} \bigg|_{X=1} = -\alpha \Theta^{S} \bigg|_{X=1} , \quad t > 0$$
(B.4)

$$\frac{1}{\alpha} \equiv \frac{\left\{\frac{L_G}{D_G} + \frac{L_P}{K_{PG}D_P} + \frac{1}{k_c}\right\}}{\left\{\frac{L_S}{K_{SG}D_S}\right\}} \equiv \frac{N_2N_6}{N_4} \left[\frac{N_1N_4}{N_3} + \frac{1}{N_7} + \frac{1}{N_5}\right]$$

$$\{\text{mass transfer resistance of the blister package}\}$$

$$(B.5)$$

 $= \frac{\{\text{mass transfer resistance of the blister package}\}}{\{\text{mass transfer resistance of the product phase}\}}$

If α is a constant (i.e., not a function of the moisture concentration), then an analytical solution to the linear boundary value problem, defined by Eqs.(B.1)-(B.4), can be represented as a Fourier series,

$$\Theta^{S}(x,t) = \sum_{n=1}^{\infty} A_n \cos(\lambda_n X) \exp(-\lambda_n^2 t) \quad , \quad 0 \le X \le 1 \quad , \quad t > 0 \, . \tag{B.6}$$

The eigenvalues are the roots to the following equation

$$\lambda_n \, \tan(\lambda_n) = \alpha \quad , \quad n = 1, 2, 3, ... \label{eq:lambda}$$
 (B.7)

the Fourier coefficients are given by

$$A_{n} = \frac{\int_{0}^{1} \cos(\lambda_{n} X) dX}{\int_{0}^{1} \left(F_{n}, F_{n}\right)} = \frac{\int_{0}^{1} \cos(\lambda_{n} X) dX}{\int_{0}^{1} \cos^{2}(\lambda_{n} X) dX} ; \quad F_{n}(X) = \cos(\lambda_{n} X)$$
(B.8)

Base case:

The following physical property data of Allen (1994) define the "base" case for the parametric study presented in Chapter 4:

$$D_S = 0.996 \times 10^{-6} \text{ cm}^2/\text{s}; D_P = 2 \times 10^{-9} \text{ cm}^2/\text{s}; \frac{D_P}{D_S} (\equiv N_4) = 0.002$$

$$L_P = 9.1 \text{ mils} = 0.023 \text{ cm} \; ; L_S = \frac{0.392}{2} = 0.196 \text{ cm} \; ; \; \frac{L_P}{L_S} (\equiv N_2) = 0.117$$
 $K_{SG} \; (\equiv N_6) = \frac{1}{a_1} \cong 16 \; ; K_{PG} \; (\equiv N_7) = 125 \; .$

If the phase resistances to moisture transport through the air gap and through the surrounding humid air are negligible, then α for the base case is approximately 0.13 inasmuch as

$$\frac{1}{\alpha} = \frac{\left\{\frac{L_{Q}}{p_{G}} + \frac{L_{P}}{K_{PG}D_{P}} + \frac{1}{k_{c}}\right\}}{\left\{\frac{L_{S}}{K_{SG}D_{S}}\right\}} = \frac{N_{2}N_{6}}{N_{4}} \left[\frac{N_{1}N_{4}}{N_{3}} + \frac{1}{N_{7}} + \frac{1}{N_{5}}\right]$$

$$\approx \frac{N_{2}N_{6}}{N_{4}N_{7}} = \frac{(0.117)(16)}{(0.002)(125)}$$

$$= 7.488 \Rightarrow \alpha = 0.133 \square 0.13$$

The first ten eigenvalues and Fourier coefficients for $\alpha = 0.1$, 0.2, and 0.3 are tabulated in Tables A.1-A.3. The following MATLAB® program was written to calculate the eigenvalues and the Fourier coefficients defined by Eq.(B.7) and Eq.(B.8), respectively.

```
bonstant(z,k)=4*sin(1(z,k))*sin(1(z,k))/(1(z,k)*(2*1(z,k)+sin(2*1(z,k)));
sum=4*sin(1(z,k))*sin(1(z,k))*exp(-(1(z,k)^2)*(j-1)*1)/(1(z,k)*(2*1(z,k)+sin(2*1(z,k))));
tum=tum+sum;
end
ans(z,j)=tum
tum=0;
tau(j)=(j-1)*1
end
end
```

Table B.1: Eigenvalues and Fourier Coefficients for the Linear PSSA-Model for $\alpha = 0.1$					
$\lambda_n \tan(\lambda_n) = \alpha$		$A_{n} = \frac{\int_{0}^{1} \cos(\lambda_{n} X) dX}{\int_{0}^{1} \cos^{2}(\lambda_{n} X) dX}$			
n	$\lambda_{\mathbf{n}}$	A _n			
1	0.31106	+1.0161			
2	3.1731	-0.01966			
3	6.2991	+0.00502			
4	9.4354	-0.00224			
5	12.574	+0.00126			
6	15.714	-0.00081			
7	18.855	+0.00056			
8	21.996	-0.00041			
9	25.137	+0.00032			
10	28.278	-0.00025			

Table B.2: Eigenvalues and Fourier Coefficients for the Linear PSSA-Model for $\alpha = 0.2$

$\lambda_n \tan(\lambda_n) = \alpha$		$A_{n} = \frac{\int_{0}^{1} \cos(\lambda_{n}X)dX}{\int_{0}^{1} \cos^{2}(\lambda_{n}X)dX}$	
n	$\lambda_{\mathbf{n}}$	A _n	
1	0.43285	+1.0311	
2	3.2039	-0.03815	
3	6.3148	+0.00998	
4	9.4459	-0.00447	
5	12.582	+0.00252	
6	15.721	-0.00162	
7	18.86	+0.00112	
8	22	-0.00083	
9	25.141	+0.00063	
10	28.281	-0.0005	

Table B.3: Eigenvalues and Fourier Coefficients for the Linear PSSA-Model for $\alpha=0.3$ $\lambda_n \tan(\lambda_n) = \alpha$ $\lambda_n = \frac{\int\limits_{-\infty}^{\infty} \cos(\lambda_n X) dX}{\int\limits_{-\infty}^{\infty} \cos^2(\lambda_n X) dX}$

		$\int_{0}^{\infty} \cos^{2}(\lambda_{n}X)dX$		
n	$\lambda_{\mathbf{n}}$	A _n		
1	0.5218	+1.045		
2	3.2341	-0.05554		
3	6.3305	+0.01484		
4	9.4565	-0.00669		
5	12.59	+0.00378		
6	15.727	-0.00242		
7	18.865	+0.00168		
8	22.005	-0.00124		
9	25.145	+0.00095		

APPENDIX C. Unsteady State Conjugate Diffusion

In this appendix, the absorption model defined in Appendix A is solved for unsteady state diffusion in both the polymer and the solid phases. The moisture concentration in the air gap is spatially uniform, but unsteady. For this situation, the three dimensionless concentration difference functions defined by Eqs.(A.1)-(A.3) satisfy the following initial boundary value problem.

Differential Equations

A material balance on the solid product phase implies thast

$$\frac{\partial \Theta^{S}}{\partial t} = \frac{\partial^{2} \Theta^{S}}{\partial X_{S}^{2}} , \quad 0 \le X_{S} \le 1 , \quad t > 0.$$
 (C.1)

A material balance on the air gap phase implies that (cf. Kim, 1992),

$$N_{\tau}^{2} \frac{d < \Theta >^{G}}{dt} = N_{P} \frac{\partial \Theta^{P}}{\partial X_{P}} \bigg|_{X_{D} = 0} - N_{\tau}^{2} N_{S} \frac{\partial \Theta^{S}}{\partial X_{S}} \bigg|_{X_{S} = 1}, \quad t > 0.$$
 (C.2)

A material balance on the polymer barrier phase implies that

$$N_{\tau}^{2} \frac{\partial \Theta^{P}}{\partial t} = \frac{\partial^{2} \Theta^{P}}{\partial X_{P}^{2}} , \quad 0 \le X_{P} \le 1 , \quad t > 0.$$
 (C.3)

The physical property parameters are related to the following dimensionless groups:

$$N_{\tau}^2 = \frac{L_P^2 / D_P}{L_S^2 / D_S} = \frac{(N_2)^2}{N_4}$$

$$N_S = \frac{V_S K_{SG}}{V_G} = \frac{V_S}{V_G} N_6$$

$$N_P \equiv \frac{V_P K_{GP}}{V_G} = \frac{V_P}{V_G} N_7$$
, $K_{GP} = K_{PG} \equiv N_7$

Initial Conditions

The initial conditions are

$$\Theta^{S}(X_{S},0) \equiv 1 , \quad 0 \le X_{S} \le 1$$
 (C.4)

$$\langle \Theta^{G} \rangle (0) = 1 \tag{C.5}$$

$$\Theta^{\mathbf{P}}(X_{\mathbf{P}},0) = 1$$
 , $0 \le X_{\mathbf{P}} \le 1$. (C.6)

Boundary Conditions

Uniformity of the concentration of water in the air gap justifies the following symmetry condition within the product tablet phase (no end effects):

$$\left. \frac{\partial \Theta^{S}}{\partial X_{S}} \right|_{X_{S}=0} = 0 \quad , \quad t > 0 \, . \tag{C.7}$$

Equilibrium and Continuity of Flux on Internal Interfaces

Thermodynamic equilibrium and a well-mixed gas phase at the SG-interface (i.e., $X_S = 1$) and the GP-interface (i.e., $X_P = 0$) require the following conditions:

$$\Theta^{S}\Big|_{X_{S}=1} = \langle \Theta \rangle^{G} (t) , \quad t > 0$$
 (C.8)

$$\Theta^{P}\Big|_{X_{P}=0} = \langle \Theta \rangle^{G} (t) , \quad t > 0$$
 (C.9)

Continuity of flux across the SG-interface and the GP-interface has been used in the application of the divergence theorem to obtain Eq. (C.2) above.

Boundary Condition at the PE-Interface

Thermodynamic equilibrium and continuity of water flux across the PE-interface at $X_P = 1$ require the following condition:

$$\frac{\partial \Theta^{\mathbf{P}}}{\partial X_{\mathbf{P}}} \bigg|_{X_{\mathbf{P}}=1} = -B\mathbf{i}^{\mathbf{m}} \Theta^{\mathbf{P}} \bigg|_{X_{\mathbf{P}}=1} , \quad t > 0.$$
 (C.10)

In the above equation,

$$Bi^{m} = \frac{k_{c}L_{p}}{K_{p}G_{p}} = \frac{Bi}{K_{p}G}. \tag{C.11}$$

An eigenfunction representation that satisfies the above initial boundary-value problem can be written as

$$\begin{pmatrix} \Theta^{S} \\ \Theta^{P} \end{pmatrix} = \sum_{n=1}^{\infty} A_{n} \begin{pmatrix} F_{n}^{S} \\ F_{n}^{P} \end{pmatrix} \exp(-\lambda_{n}^{2}t)$$
(C.12)

$$F_n^S(X_S) = B_{1n}^S \sin(\lambda_n X_S) + B_{2n}^S \cos(\lambda_n X_S)$$
 (C.13)

$$F_n^P(X_P) = B_{1n}^P \sin(N_\tau \lambda_n X_P) + B_{2n}^P \cos(N_\tau \lambda_n X_P)$$
 (C.14)

Using (C.12) through (C.14) with the boundary condition (C.7) through (C.10) and the air gap material balance (Eq.(C.2)), it follows that

$$F_n^S(1) = F_n^P(0)$$
 (C.15)

$$B_{1n}^{S} = 0$$
 (C.16)

$$\frac{B_{2n}^{P}}{B_{2n}^{S}} = \cos(\lambda_n) \tag{C.17}$$

$$\frac{B_{ln}^{P}}{B_{2n}^{P}} = \frac{(N_{\tau}\lambda_{n} \tan(N_{\tau}\lambda_{n}) - Bi^{m})}{(N_{\tau}\lambda_{n} + Bi^{m} \tan(N_{\tau}\lambda_{n}))} \xrightarrow{Bi^{m} \to \infty} \frac{-1}{\tan(N_{\tau}\lambda_{n})}.$$
 (C.18)

From Eqs.(C.8) and (C.12), it follows that

$$<\Theta>^{G}(t) = \Theta^{S}\Big|_{X_{S}=1} = \sum_{n=1}^{\infty} A_{n} e^{-\lambda_{n}^{2} t} B_{2n}^{S} \cos \lambda_{n} , t > 0.$$
 (C.19)

Therefore,

$$\frac{d < \Theta >^{G}(t)}{dt} = -\sum_{n=1}^{\infty} \lambda_{n}^{2} A_{n} e^{-\lambda_{n}^{2} t} B_{2n}^{S} \cos \lambda_{n} , \quad t > 0$$
 (C.20)

Eigenvalues

Inserting Eqs.(C.12) through (C.19) into (C.2) yields the following equation for the eigenvalues:

$$\lambda_{n} + N_{S} \tan(\lambda_{n}) + \frac{N_{P}}{N_{\tau}} \frac{(N_{\tau}\lambda_{n} \tan(N_{\tau}\lambda_{n}) - Bi^{m})}{(N_{\tau}\lambda_{n} + Bi^{m} \tan(N_{\tau}\lambda_{n}))} = \Im(\lambda_{n}) = 0$$
 (C.21)

Eq. (C.21) reduces to Eq. (B.7) when the pseudo steady state is applied to the polymer phase. The development of the same is discussed in Appendix F.

Fourier Coefficients

The eigenfunctions satisfy the following boundary value problem:

$$\frac{dF_{n}^{S}}{dX_{S}^{2}} = -\lambda_{n}^{2}F_{n}^{S} , \quad 0 \le X_{S} \le 1$$
 (C.22)

$$\frac{dF_{n}^{P}}{dX_{p}^{2}} = -N_{\tau}^{2}\lambda_{n}^{2}F_{n}^{P} \quad , \quad 0 \le X_{p} \le 1$$
 (C.23)

$$-N_{\tau}^{2}\lambda_{n}^{2}F_{n}^{S}\Big|_{X_{S}=1} = N_{P}\frac{dF_{n}^{P}}{dX_{P}}\Big|_{X_{P}=0} -N_{\tau}^{2}N_{S}\frac{dF_{n}^{S}}{dX_{S}}\Big|_{X_{S}=1}$$
(C.24)

$$-N_{\tau}^{2}\lambda_{n}^{2}F_{n}^{P}\Big|_{X_{P}=0} = N_{P}\frac{dF_{n}^{P}}{dX_{P}}\Big|_{X_{P}=0} -N_{\tau}^{2}N_{S}\frac{dF_{n}^{S}}{dX_{S}}\Big|_{X_{S}=1}$$
(C.25)

Equation (C.22) for a value n = m gives

$$\frac{dF_{m}^{S}}{dX_{S}^{2}} = -\lambda_{m}^{2} F_{m}^{S} \quad , \quad 0 \le X_{S} \le 1$$
 (C.26)

Thus, it follows from Eqs. (C.22) and (C.26) that

$$(F_{m}^{S} \frac{dF_{n}^{S}}{dX_{S}}) \bigg|_{X_{S}=1} - (F_{n}^{S} \frac{dF_{m}^{S}}{dX_{S}}) \bigg|_{X_{S}=1} = -(\lambda_{n}^{2} - \lambda_{m}^{2}) \int_{0}^{1} F_{n}^{S} F_{m}^{S} dX_{S}$$
 (C.27)

The polymer phase provides a similar result inasmuch as

$$(F_n^P \frac{dF_m^P}{dX_P}) \bigg|_{X_P = 0} - (F_m^P \frac{dF_m^P}{dX_P}) \bigg|_{X_P = 0} = -(\lambda_n^2 - \lambda_m^2) N_\tau^2 \int_0^1 F_n^p F_m^p dX_p$$
 (C.28)

Multiplying Eq.(C.24) by $F_m^S(1)$ and Eq.(C.24) by $F_n^S(1)$ and subtracting the resulting equations and using (C.15) yields

$$-N_{\tau}^{2}(\lambda_{n}^{2}-\lambda_{m}^{2})F_{n}^{S}\Big|_{X_{S}=1}F_{m}^{P}\Big|_{X_{P}=0}=N_{P}\left[F_{m}^{P}\frac{dF_{n}^{P}}{dX_{P}}\Big|_{X_{P}=0}-F_{n}^{P}\frac{dF_{m}^{P}}{dX_{P}}\Big|_{X_{P}=0}\right]$$

$$-N_{\tau}^{2}N_{s}\left[F_{m}^{S}\frac{dF_{n}^{S}}{dX_{S}}\Big|_{X_{S}=1}-F_{n}^{S}\frac{dF_{m}^{S}}{dX_{S}}\Big|_{X_{S}=1}\right]$$
(C.29)

Combining Eqs.(C.27), (C.28), and (C.29) shows that the eigenfuctions satisfy the following condition:

$$N_{S} \int_{0}^{1} F_{n}^{S}(X_{S}) F_{m}^{S}(X_{S}) dX_{S} + N_{P} \int_{0}^{1} F_{n}^{P}(X_{P}) F_{m}^{P}(X_{P}) dX_{P} + F_{n}^{S}(1) F_{m}^{P}(0) = 0$$
 (C.30)

The moisture distribution in the solid phase can be represented as

$$\Theta^{S} = \sum_{n=1}^{\infty} A_n F_n^S e^{-\lambda_n^2 t}$$
 (C.31)

Therefore, for t = 0, it follows that

$$1 = \sum_{n=1}^{\infty} A_n F_n^{S}(X_S)$$
 (C.32)

For $X_S = 1$, Eq.(C.32) implies that

$$1 = \sum_{n=1}^{\infty} A_n F_n^{S}(1) . (C.33)$$

The moisture distribution in the polymer barrier phase can be represented as

$$\Theta^{P} = \sum_{n=1}^{\infty} A_n F_n^P e^{-\lambda_n^2 t}$$
 (C.34)

Therefore, for t = 0, it follows that

$$1 = \sum_{n=1}^{\infty} A_n F_n^P(X_P).$$
 (C.35)

For $X_P = 0$, Eq.(C.35) implies that.

$$1 = \sum_{n=1}^{\infty} A_n F_n^{P}(0).$$
 (C.36)

Multiplying (C.32) and (C.35) by F_m^S and F_m^P , respectively, and integrating yields

$$\int_{0}^{1} F_{m}^{S} dX_{S} = A_{m} \int_{0}^{1} F_{m}^{S} F_{m}^{S} dX_{S} + \sum_{n \neq m} A_{n} \int_{0}^{1} F_{m}^{S} F_{n}^{S} dX_{S}$$
(C.37)

$$\int_{0}^{1} F_{m}^{P} dX_{P} = A_{m} \int_{0}^{1} F_{m}^{P} F_{m}^{P} dX_{P} + \sum_{n \neq m} A_{n} \int_{0}^{1} F_{m}^{P} F_{n}^{P} dX_{P}$$
(C.38)

Eqs. (C.37) and (C.38) can be combined with the result that

$$N_{S} \int_{0}^{1} F_{m}^{S} dX_{S} + N_{P} \int_{0}^{1} F_{m}^{P} dX_{P} = A_{m} [N_{S} \int_{0}^{1} F_{m}^{S} F_{m}^{S} dX_{S} + N_{P} \int_{0}^{1} F_{m}^{P} F_{m}^{P} dX_{P}]$$

$$- \sum_{n \neq m} A_{n} F_{n}^{S}(1) F_{m}^{P}(0)$$
(C.39)

Eqs. (C.36) and (C.15) imply that

$$F_{\mathbf{m}}^{\mathbf{p}}(0) = A_{\mathbf{m}} F_{\mathbf{m}}^{\mathbf{p}}(0) F_{\mathbf{m}}^{\mathbf{S}}(1) + \sum_{\mathbf{n} \neq \mathbf{m}} A_{\mathbf{n}} F_{\mathbf{n}}^{\mathbf{p}}(0) F_{\mathbf{m}}^{\mathbf{S}}(1) . \tag{C.40}$$

Combining Eqs.(C.40) and (C.39) gives the following equation for the Fourier coefficients:

$$A_{m} = \frac{\frac{1}{N_{S} \int_{S}^{S} F_{m}^{S}(X_{S}) dX_{S} + N_{P} \int_{S}^{P} F_{m}^{P}(X_{P}) dX_{P} + F_{m}^{S}(1)}{\frac{1}{N_{S} \int_{S}^{S} F_{m}^{S}(X_{S}) F_{m}^{S}(X_{S}) dX_{S} + N_{P} \int_{S}^{P} F_{m}^{P}(X_{P}) F_{m}^{P}(X_{P}) dX_{P} + F_{m}^{S}(1) F_{m}^{P}(0)}}$$
(C.41)

The first ten eigenvalues and Fourier coefficients for ???? are tabulated in Tables C.1-C.?. The following MATLAB® program was written to calculate the eigenvalues and the Fourier coefficients for the conjugate mass transfer problem developed in this appendix (i.e., see Eqs.(C.21) and (C.41) above).

```
for z=1:6
y=0.02;
for i=1:10
Ns = 12:
Np = (z * 4) - 1;
Nt=3;
Bi = 100000:
while (-1)^{(i)} * (y+Ns*tan(y)+Np/Nt*(Nt*y*tan(Nt*y)-
Bi)/(Nt*y+(Bi*tan(Nt*y))))>=0
    y=y+0.00001;
end
1(z, i) = y;
y=y+0.0001;
end
end
for z=1:6
for j=2:101
    ans=0;
    ans2=0;
for i=1:10
t = (j-1) *1;
Ns=12;
Np = (z * 4) - 1;
Nt=3;
Bi=100000;
a(z,i) = (Nt*l(z,i)*tan(Nt*l(z,i)) -
Bi)/(Nt*l(z,i)+Bi*tan(l(z,i)*Nt));
num(z,i) = Ns * tan(l(z,i))/l(z,i) + Np/(Nt * l(z,i)) * (a(z,i) * (1-
cos(Nt*l(z,i)))+sin(Nt*l(z,i)))+1;
denom(z,i)=Ns/((cos(l(z,i)))^2)/(4*l(z,i))*(2*l(z,i)+sin(2*))
l(z,i)) + Np*(((a(z,i)*a(z,i))+1)/2-
(a(z,i)*cos(2*Nt*l(z,i))/(2*Nt*l(z,i)))-(((a(z,i)*a(z,i))-
1) *\sin(2*Nt*1(z,i))/(4*Nt*1(z,i))) + a(z,i)/(2*Nt*1(z,i))) + 1;
An (z,i) = num(z,i) / denom(z,i);
sum(z,i) = An(z,i) * cos(l(z,i)*1.0) / (cos(l(z,i))) * exp(-
(1(z,i))^2*t)
sum2(z,i) = An(z,i) * (a(z,i) * sin(Nt*1(z,i)*0) + cos(Nt*1(z,i)*0)
)*exp(-(l(z,i))^2*t)
ans=ans+sum(z,i);
ans2=ans2+sum2(z,i);
end
```

```
ans1(z,j)=ans ans3(z,j)=ans2 ans1(z,1)=1; ans3(z,1)=1; tau(j)=(j-1)*1; end t(z)=\log(An(z,1)*tan(l(z,1))*2/l(z,1))/(l(z,1))^2; end
```

APPENDIX D. Problem Setup for the Non-Linear PSSA Model

The non-linear PSSA-model was solved numerically. A GAB-isotherm at the product-gas interface makes the boundary value problem non-linear (see Sections 3.8 and 3.9). The setup of the computational problem using COMSOL MULTIPHYSICS® is described in this appendix.

Differential Equation (dimensional)

$$\frac{\partial C^{S}}{\partial \hat{t}} = D_{S} \frac{\partial^{2} C^{S}}{\partial \hat{x}^{2}} , \quad 0 \le \hat{X} \le L_{S} , \quad \hat{t} > 0$$
 (D.1)

Initial Condition

$$C^{S}(\hat{X}, 0) = C_{0}^{S}$$
 , $0 \le \hat{X} \le L_{S}$ (D.2)

Symmetry Boundary Condition

As indicated by Figure 3.1, the boundary condition on the symmetry plane in the product tablet is

$$\frac{\partial C^{S}}{\partial \hat{X}}\Big|_{\hat{X}=0} = 0 \quad , \quad \hat{t} > 0 \tag{D.3}$$

Boundary Condition at the SG-Interface

A pseudo-steady state approximation for the moisture flux across the air gap and the polymer barrier yields the following condition at the SG-interface:

$$D_{S} \frac{\partial C^{S}}{\partial \hat{X}} \bigg|_{\hat{X} = L_{S}} = + k_{eff} \left(C^{E} - C^{G} \right|_{\hat{X} = L_{S}}), \quad \hat{t} > 0.$$
 (D.4a)

The effective mass transfer coefficient k_{eff} in Eq.(D.4a) is defined as follows

$$\frac{1}{k_{\text{eff}}} = \frac{L_{\text{G}}}{D_{\text{G}}} + \frac{L_{\text{P}}}{K_{\text{PG}}D_{\text{P}}} + \frac{1}{k_{\text{c}}}.$$
(D.4b)

With

$$\begin{split} & M(X,t) \equiv C^{S}(\hat{X},\hat{t})/\rho_{S} = M_{eq}^{S} - (M_{eq}^{S} - M_{o}^{S})\Theta^{S}(X,t) \\ & A_{w}(L_{S},t) \equiv C^{G}(L_{S},\hat{t})/C_{eq}^{G} = < C^{G} > (\hat{t})/C_{eq}^{G} \quad , \quad A_{w}^{E} \equiv C^{E}/C_{eq}^{G} \\ & X \equiv \hat{X}/L_{S} \end{split} \tag{D.4c}$$

Eq.(D.4a) can be re-written as

$$\left. \frac{\partial M}{\partial X} \right|_{X=1} = + \tilde{\alpha} \left(A_{W}^{E} - A_{W} \right|_{X=1}) , \quad \tilde{\alpha} \equiv \frac{k_{eff} L_{S} C_{eq}^{G}}{D_{S} \rho_{S}} , \quad C_{eq}^{G} = 18 \frac{p_{water}}{R_{g} T}. \quad (D.4d)$$

The nonlinear PSSA-model is defined by the following boundary value problem:

$$\frac{\partial M}{\partial t} = \frac{\partial^2 M}{\partial X^2} \quad , \quad 0 \le X \le 1$$
 (D.5)

$$\left. \frac{\partial \mathbf{M}}{\partial \mathbf{X}} \right|_{\mathbf{X} = \mathbf{0}} = 0 \tag{D.6}$$

$$\frac{\partial M}{\partial X}\bigg|_{X=1} = +\tilde{\alpha} \left(A_w^E - A_w \bigg|_{X=1} \right) \qquad . \tag{D.7}$$

The GAB-isotherm at the PE-interface relates the mass ratio to the relative humidity $A_{\mathbf{W}}$ as follows (see Chapter 2):

$$M|_{X=1} = \frac{A_{w}|_{X=1}}{a_{3}(A_{w}|_{X=1})^{2} + a_{2}(A_{w}|_{X=1}) + a_{1}}.$$
 (D.8)

Eqs.(D.5) through (D.8) were solved using a finite element code supported by COMSOL MULITIPHYSICS®. The results are reported in Chapters 3 and 4.

In COMSOL MULTIPHYSICS® 3.3, under the model library for 1D space dimension. The user option, "Mass Balance - Diffusion - Transient Analysis", was selected under the chemical engineering module. Using the "draw" menu, a one dimensional flat plate of unit thickness (dimensionless units) was drawn. The faces of the plate were marked to identify the boundaries. The model constants, initial values, and properties of each boundary were set in the "Physics" menu and the FEM grid was generated with the default values (15 mesh elements) and a time step of 0.1 was selected. The boundary value problem was solved for the time scale desired.

Eq. (D.8) was rearranged to obtain an explicit equation for $A_{\mathbf{W}}$ in terms of M. For a given value of M, Eq.(D.8) is a quadratic equation for $A_{\mathbf{W}}$:

$$a_3 M A_w^2 + (a_2 M-1) A_w + a_1 M = 0.$$
 (D.9)

The first and second GAB-coefficients are positive, and the third coefficient is negative: $a_1 > 0$, $a_2 > 0$, and $a_3 < 0$. Therefore, the positive root of Eq.(D.9) is

$$A_W = \frac{+(a_2 M - 1) + \sqrt{(a_2 M - 1)^2 + 4|a_3|a_1 M^2}}{2|a_3|M}, \text{ for } X = 1.$$
 (D.10)

Eq.(D.10) was substituted into (D.7) to give a non-linear boundary condition at the solid/air gap interface consistent with thermodynamic equilibrium and continuity of moisture flux at the interface.

Base Case:

The physical property data of Allen (1994) are summarized in Table 4.1 above. The following values are taken as the "base" case for the parametric study presented in Chapter 4:

$$D_S = 0.996 \times 10^{-6} \text{ cm}^2/\text{s}$$
, $L_S = \frac{0.392}{2} = 0.196 \text{ cm}$

$$D_P = 2 \times 10^{-9} \text{ cm}^2/\text{s}$$
 , $L_P = 9.1 \text{ mils} = 0.023 \text{ cm}$

$$\rho_S = 1.39 \text{ g/(cm}^3)$$
, $K_{PG} = 125$

$$C_{eq}^G = 18 \frac{p_{water}}{R_g T} = 18 \frac{?}{??} = ?0.028 \text{ g/(cm}^3)$$

$$k_{eff} = \frac{1}{\frac{L_O}{D_G} + \frac{L_P}{K_{PG}D_P} + \frac{1}{K_C}}$$

$$\tilde{\alpha} = \frac{k_{eff} L_{S} C_{eq}^{G}}{D_{S} \rho_{S}} = \frac{N_{4}}{N_{2}} \frac{C_{eq}^{G}}{\rho_{S}} = \frac{(0.002)}{(0.117)} \frac{(0.028)}{(1.39)} \approx 0.038$$

APPENDIX E. Absorption: Flat Plate Geometry and Large Biot Numbers

The absorption of moisture in a flat plate of thickness $2L_S$ surrounded by humid air at a relative humidity of A_W^E is described by the following boundary value problem, which is just a special case of the problem described in Appendix A. The purpose of this appendix is to define the boundary value problem that governs the absorption experiments conducted by Allen(1994) on "flat plate drug tablets and "flat" plate polymer barriers. These experiments are designed to measure the thermodynamic adsorption isotherms and the diffusion coefficients of the three materials in the blister package. A microbalance is used to directly measure the mass of water absorbed per mass of dry solids as a function of time. Allen's experiments were designed so that 1) the convective mass transfer coefficient k_C was large compared with a characteristic velocity for diffusion through the solid phase (i.e., large Biot number); and, 2) the surrounding moisture concentration in the humid air was the same over the entire surface of the solid and did not change with time.

Solid Phase --- Boundary Value Problem (drug tablets or polymer barriers)

With $M = C(\hat{X}, \hat{t})/\rho$ equal to the mass of water absorbed per unit mass of dry solid, it follows directly from the discussion in Appendix B (and elsewhere in this thesis) that

$$\frac{\partial M}{\partial t} = \frac{\partial^2 M}{\partial X^2} \quad , \quad 0 \le X \le 1 \quad , \quad t > 0 \quad , \quad t \equiv \frac{\hat{t} D^2}{L^2} \quad , \quad X \equiv \frac{\hat{X}}{L} \, . \tag{E.1}$$

$$M(X,0) \equiv C(X,0)/\rho = M_0$$
 (constant) , $0 \le X \le 1$ (E.2)

$$\left. \frac{\partial \mathbf{M}}{\partial \mathbf{X}} \right|_{\mathbf{X} = 0} = 0, \quad \mathbf{t} > 0 \tag{E.3}$$

$$M(l,t) = \Im(A_{W}(l,t)) = \begin{cases} \tilde{K}_{SG} A_{W} = \text{constant} , & \text{linear isotherm} \\ \frac{A_{W}}{a_{3}A_{W}^{2} + a_{2}A_{W} + a_{1}} = \text{constant} , & \text{GAB-isotherm} \end{cases}$$
(E.4)

A Fourier series representation of a solution to Eqs.(E.1)-(E.4), which is equivalent to the special case $\alpha = \infty$ (see Appendix B above), is given by (cf. Eq.(B.6):

$$M(X,t) = M_1 - (M_1 - M_0) \sum_{n=0}^{\infty} A_n \cos(\lambda_n X) e^{-\lambda_n^2 t}, \quad 0 \le X \le 1 \quad , \quad t > 0.$$
 (E.5)

$$cos(\lambda_n) = 0$$
 , $\lambda_n = \frac{(2n+1)\pi}{2}$, $n = 0,1,2,3,...$ (E.6)

The Fourier coefficients are defined by Eq.(B.8) for $\alpha = \infty$:

$$A_{n} = \frac{\int_{0}^{1} \cos(\lambda_{n} X) dX}{\int_{0}^{1} \cos^{2}(\lambda_{n} X) dX} = \frac{4 \sin(\lambda_{n})}{2 \lambda_{n} + \sin(2\lambda_{n})} . \tag{E.7}$$

The volume average of Eq.(E.5) gives (see p. 45, Crank, 1956):

$$M_{t} = \int_{0}^{1} M(X,t) dX = M_{1} - (M_{1} - M_{0}) \sum_{n=0}^{\infty} A_{n} \left[\int_{0}^{1} \cos(\lambda_{n} X) dX \right] e^{-\lambda_{n}^{2} t}$$

$$= M_{1} - (M_{1} - M_{0}) \frac{8}{\pi^{2}} \sum_{n=0}^{\infty} \frac{1}{(2n+1)^{2}} e^{-\lambda_{n}^{2} t}$$
(E.8)

Eq.(E.8) was used by Allen (1994) to estimate the thermodynamic parameters in Eq.(E.4) by measuring M_1 for $t \to \infty$ for different values of A_W . The diffusion coefficient was

also estimated by fitting Eq.(E.8) to the unsteady state absorption data. The following examples (and many more) were reported by Allen.

Deltasone ® - drug tablet

$$\begin{split} L_{drug} &= 0.196 \text{ cm} \quad \text{(half thickness)} \\ M_{O} &= 0 \quad \text{(dry solid)} \\ A_{W} &= 0.873 \text{ RH} \\ M_{1} &= 1.976 \frac{\text{g water}}{100 \text{ g dry solid}} \\ D_{drug} &= 0.996 \times 10^{-6} \text{ cm}^{2} / \text{s} \end{split}$$

PVC--- polymer barrier

$$\begin{split} L_{PVC} &= 0.0095 \text{ cm} \quad \text{(half thickness)} \\ M_{O} &= 0 \quad \text{(dry solid)} \\ A_{W} &= 0.77 \text{ RH} \\ M_{1} &= 0.133 \frac{\text{g water}}{100 \text{ g dry solid}} \\ D_{PVC} &= 5.04 \times 10^{-9} \text{ cm}^{2} / \text{s} \end{split}$$

ACLAR® --- polymer barrier

$$L_{ACLAR} = 0.0020 \text{ cm}$$
 (half thickness)
 $M_0 = 0$ (dry solid)
 $A_W = 0.58 \text{ RH}$
 $M_1 = 0.121 \frac{\text{g water}}{100 \text{ g dry solid}}$
 $D_{ACLAR} = 7.03 \times 10^{-10} \text{ cm}^2/\text{s}$

Figures (2.3)-(2.5) in Chapter 2 compare the experimental data reported by Allen (1994) and the theoretical result given by Eq.(E.8) for the three diffusivities given above. This type of information is used in Chapters 3 and 4 to simulate the absorption of moisture in a blister package.

APPENDIX F. Justification of PSSA-Model for Linear Adsorption

PSSA-model

In this appendix, the PSSA-model developed in Appendix B is compared with the exact solution of the conjugate mass transfer problem developed in Appendix C. Application of the pseudo-steady state assumptions to Eq.(C.2) and Eq.(C.3) implies that

$$N_{\tau}^{2} \frac{d < \Theta^{G} >}{dt} = N_{P} \frac{\partial \Theta^{P}}{\partial X_{P}} \bigg|_{X_{P} = 0} - N_{\tau}^{2} N_{S} \frac{\partial \Theta^{S}}{\partial X_{S}} \bigg|_{X_{S} = 1} \approx 0, \quad t > 0$$
 (F.1)

$$N_{\tau}^{2} \frac{\partial \Theta^{P}}{\partial t} = \frac{\partial^{2} \Theta^{P}}{\partial X_{P}^{2}} \cong 0 \quad , \quad 0 \le X_{P} \le 1 \quad , \quad t > 0$$
 (F.2)

Because $\Theta^S(1,t)=<\Theta^G>(t)=\Theta^P(0,t)$ and (for $Bi=\infty$) $\Theta^P(1,t)=0$, Eq.(F.2) implies that

$$\frac{\partial \Theta^{\mathbf{P}}}{\partial X_{\mathbf{P}}} \bigg|_{X_{\mathbf{P}}=0} = \frac{\Theta^{\mathbf{P}}(1,t) - \Theta^{\mathbf{P}}(0,t)}{1 - 0} = -\Theta^{\mathbf{P}}(0,t) = -\Theta^{\mathbf{S}}(1,t) , \quad t > 0.$$
(F.3)

Therefore, the PSSA-boundary condition at the SG-interface follows by combining Eqs.(F.1) and (F.3):

$$\left. \frac{\partial \Theta^{S}}{\partial X_{S}} \right|_{X_{S}=1} = -\frac{N_{P}}{N_{\tau}^{2} N_{S}} \Theta^{S}(1,t) \qquad , \qquad \alpha = \frac{N_{P}}{N_{\tau}^{2} N_{S}} \quad , \quad t > 0 \, . \tag{F.4}$$

Eq.(F.4) is a special case for which $Bi = \infty$ and the resistance to mass transfer across the air gap due to accumulation of moisture is neglected (see approximation (F.1) above). Therefore, the absorption of moisture into the solid product phase is governed by Eq.(F.4) and the following two conditions:

$$\frac{\partial \Theta^{S}}{\partial t} = \frac{\partial^{2} \Theta^{S}}{\partial X_{S}^{2}} , \quad 0 \le X_{S} \le 1 , \quad t > 0$$
 (F.5)

$$\left. \frac{\partial \Theta^{S}}{\partial X_{S}} \right|_{X_{S}=0} = 0 \tag{F.6}$$

The solution to Eq.(F.5) subject to Eqs.(F.4) and (F.6) has been developed in Appendix B. In what follows, the exact solution of the linear conjugate absorption problem developed in Appendix C is compared with the corresponding exact solution of the linear PSSA-model. The following set of physical property parameters from Allen's thesis (Allen, 1994) is used in the comparison.

Base Case

$$L_S = 0.196 \; \text{cm}$$
 , $\; L_G = 0.258 \; \text{cm}$, $\; L_P = 0.0023 \; \text{cm}$

$$D_S = 0.1179 \times 10^{-5} \text{ cm}^2/\text{s}$$
, $D_P = 2 \times 10^{-9} \text{ cm}^2/\text{s}$

$$K_{SG} = \frac{1}{a_3} = \frac{1}{0.064} = 16, K_{PG} = 125$$

$$\frac{V_S}{V_G} = \frac{L_S}{L_G} = \frac{0.196}{0.258} = 0.76$$

$$\frac{V_P}{V_G} = \frac{L_P}{L_G} = \frac{0.0023}{0.258} = 0.0089$$

$$\frac{L_P}{L_S} = \frac{0.0023}{0.196} = 0.0117$$

$$\frac{D_S}{D_P} = \frac{0.1179 \times 10^{-5}}{2 \times 10^{-9}} = 590$$

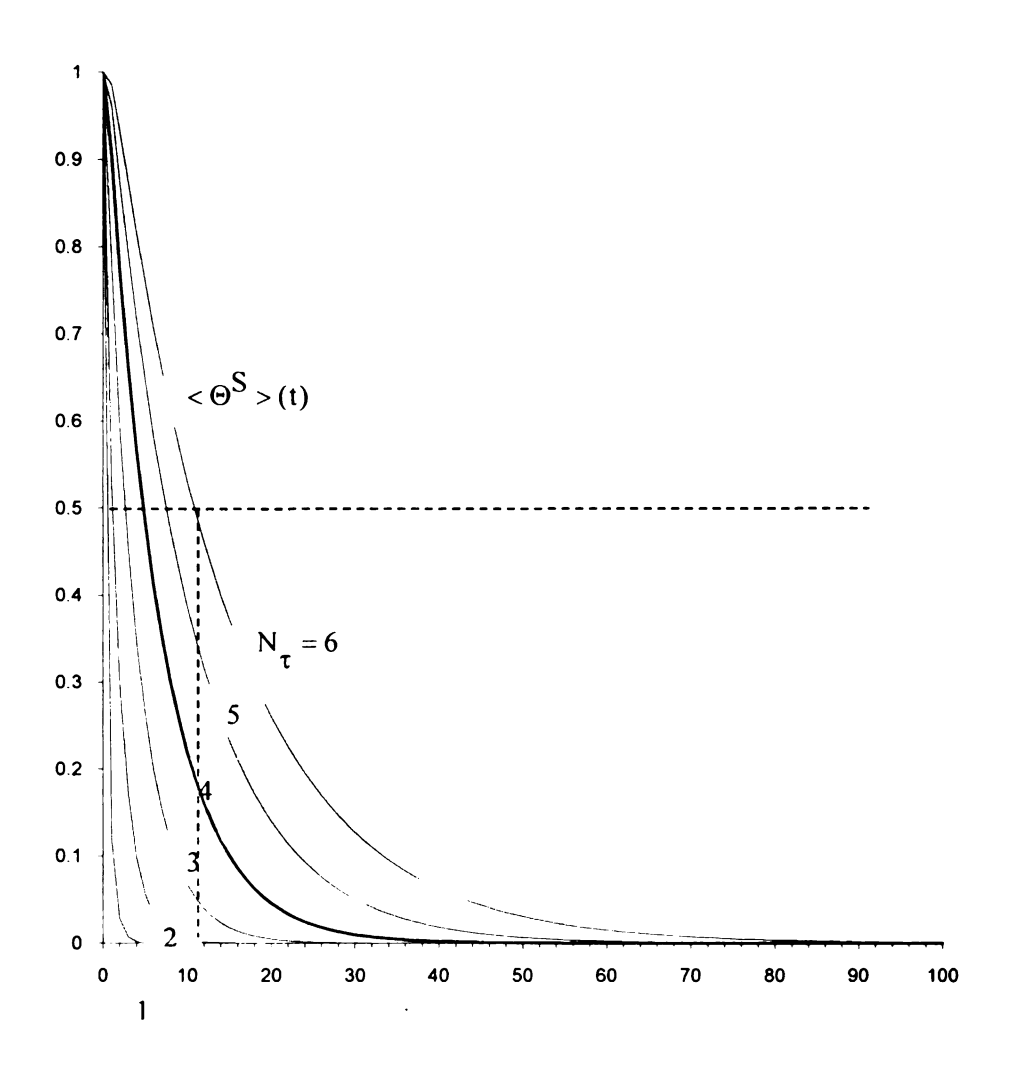
$$N_{\tau}^2 = (\frac{L_P}{L_S})^2 \frac{D_S}{D_P} = (0.0117)^2 \times 590 = 0.0808 \Rightarrow N_{\tau} = \sqrt{0.0808} \cong 0.2842$$

$$N_S = \frac{V_S}{V_G} K_{SG} = \frac{L_S}{L_G} K_{SG} = (0.76)(16) \cong 12$$

$$N_P = \frac{V_P}{V_G} K_{PG} = \frac{L_P}{L_G} K_{PG} = (0.0089)(125) \cong 1.1$$

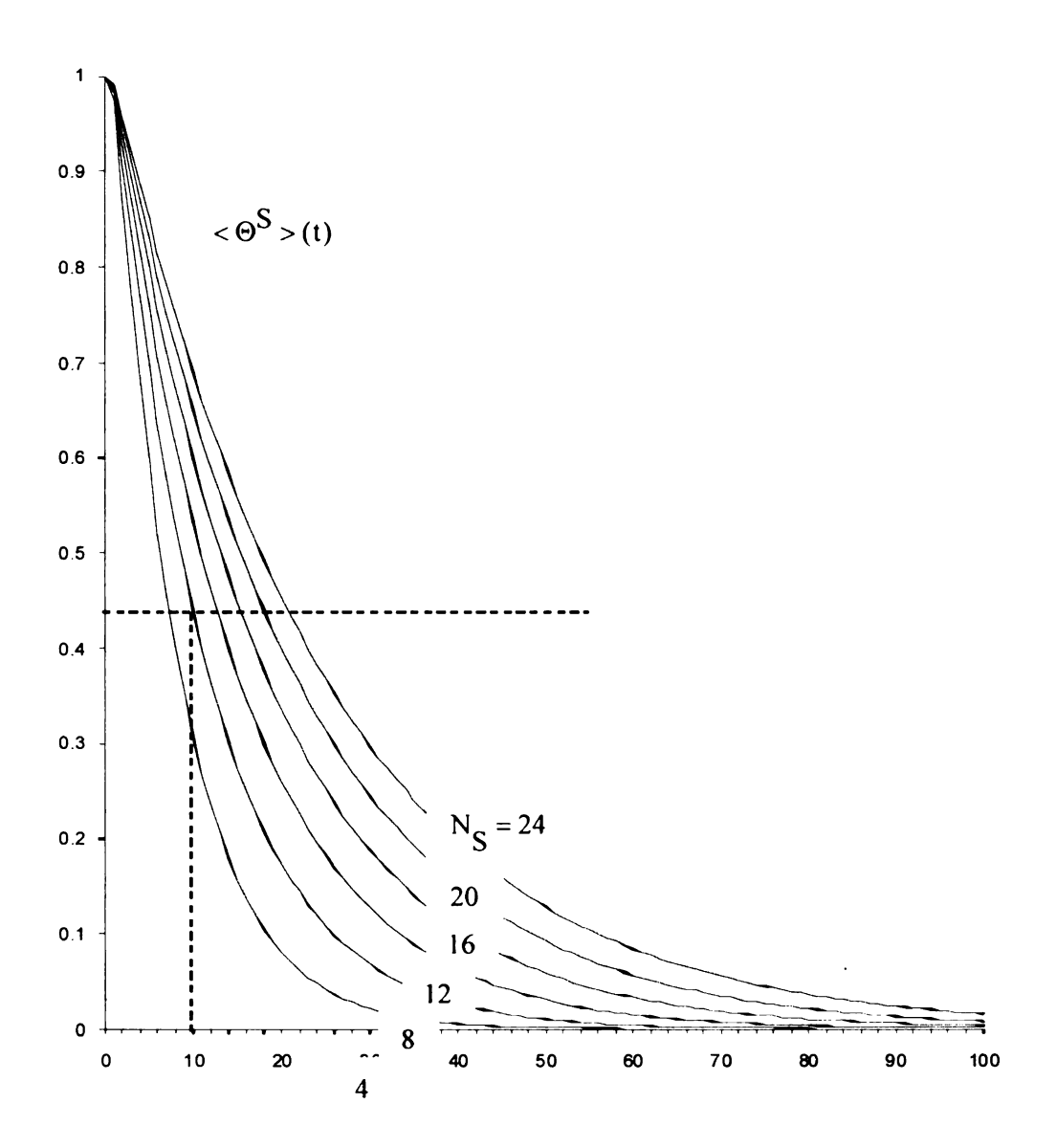
$$\alpha = \frac{N_P}{N_\tau^2 N_S} = \frac{(1.1)}{(0.0808)(12)} \cong 1.13$$

Figures F.1, F.2 and F.3 show the relaxation of the PQI-function for different values of the dimensionless groups: N_{τ} , N_{S} and N_{P} . For N_{τ} =0.28, N_{S} =12, and N_{P} =1.1, the PQI-time (defined as $<\Theta^{S}>(t_{c})$ =0.5) predicted by the linear conjugate absorption model is about 11 L_{S}^{2}/D_{S} , which is about 100 hours for the problem defined above. For the linear PSSA-model, the PQI-time is about $8L_{S}^{2}/D_{S}$ (see Figure 4.1 in Chapter 4).



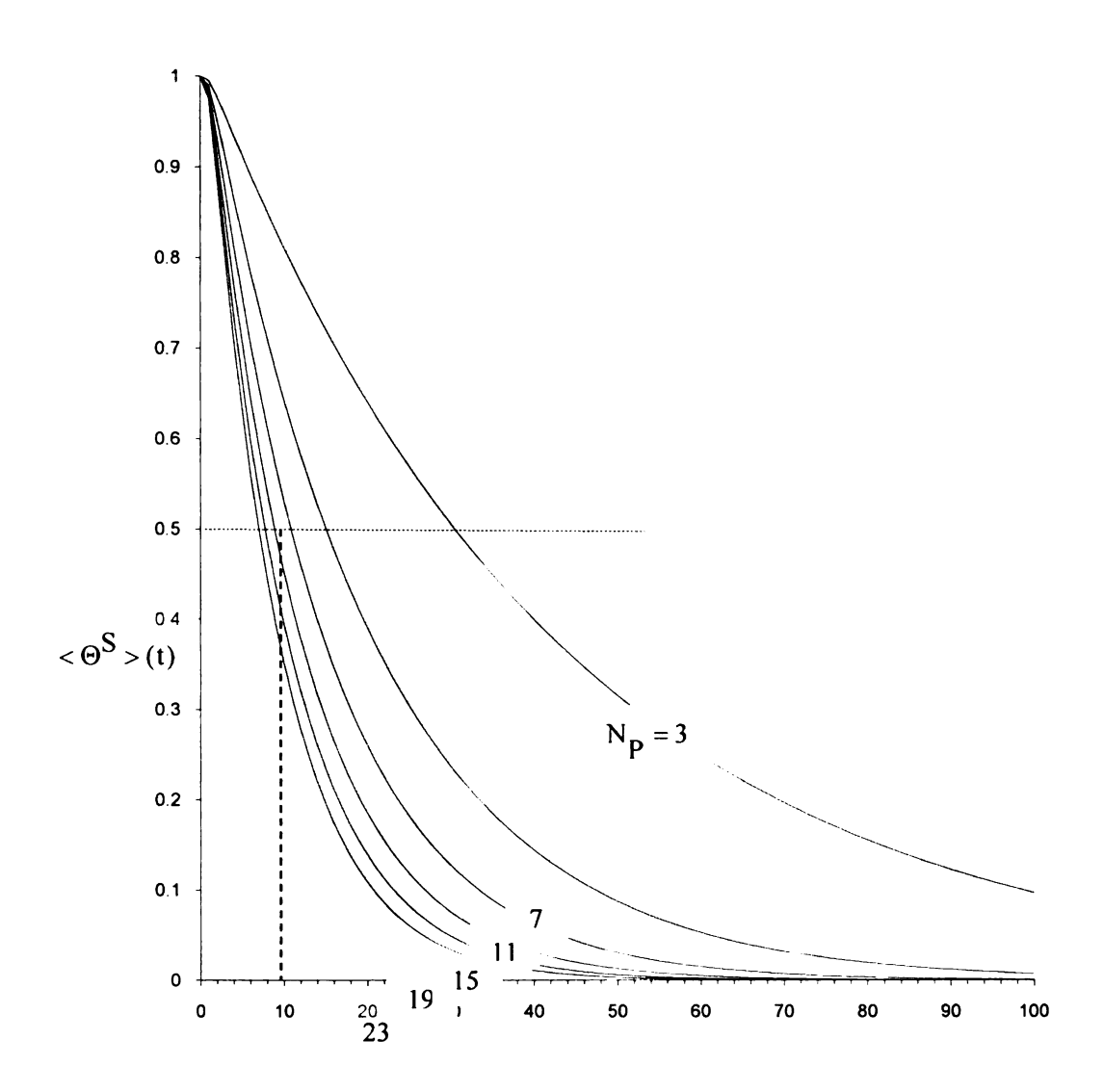
$$t = \frac{\hat{t}D_S}{L_S^2}$$

Figure F.1 Effect of N_{τ} on the PQI-function (N_{S} =12, N_{P} =11).



$$t = \frac{\hat{t}D_S}{L_S^2}$$

Figure F.2 Effect of N_S on the PQI-function ($N_P=11, N_{\tau}=3$).



$$t = \frac{\hat{t}D_S}{L_S^2}$$

Figure F.3 Effect of N_P on the PQI-function (N_{τ} =3, N_S =12).

Table F.1 Effect of N_S, N_P & N_T on the Shelf-Life for the Linear Model $<\Theta^S>(t_c)\equiv\Theta_c^S=0.5~;~\hat{t}_c=t_cL_S^2/D_S~;~L_S^2/D_S\cong11~hours$

NS	Np	Ν _τ	t _C Exact	$\alpha = \frac{Np}{N_{\tau}^2 N_S}$	t _C PSSA
12	11	1	1	1.1	1
12	11	3	11	0.12	8
12	11	6	44	0.03	51
12	3	3	31	0.04	46
12	11	3	11	0.12	8
12	23	3	7	0.24	3
4	11	3	5	0.44	5
12	11	3	11	0.12	8
24	11	3	20	0.06	25

REFERENCES

REFERENCES

- Ahlneck C.and Zografi G., 1990, "The molecular basis of moisture effects on the physical and chemical stability of drugs in the solid state", *Int. J. Pharm.*, 62, 87-95(1990).
- Allen P.J., 1994, "Measuring the Sorption and Diffusion of Water in a Moisture Sensitive Product for Use in Shelf Life Simulation", Master of Science Thesis, Michigan State University.
- Anderson G. and Scott M., 1991, "Determination of Product Shelf Life and Activation Energy for Five Drugs of Abuse", *Clin. Chem.*, 37(3), 398-402.
- Anderson R.B., 1946, "Modifications of the Brunauer, Emmett and Teller Equation", J. Am. Chem. Soc., 68, 686-91.
- Badawy S.I.F., Gwaronski A.J. and Alvarez F.J., 2001, "Application of sorption-desorption moisture transfer modeling to the study of chemical stability of a moisture sensitive drug product on different packaging configurations, *J. Pharm. Sci.*, 223, 1-13.
- Bell L.N. and Labuza T.P., 2000, "Moisture sorption: practical aspects of isotherm measurement and use", St. Paul, Minn.: American Association of Cereal Chemists.
- Bird R.B., Stewart W.E. and Lightfoot E.N., 2002, "Transport Phenomena", New York: J. Wiley.
- Bischoff K.B., 1963, "Accuracy of the pseudo steady state approximation for moving boundary diffusion problems", *Chem. Eng. Sci.*, 18, 711-713.
- Bischoff K.B., 1965, "Further comments on the pseudo steady state approximation for moving boundary diffusion problems", *Chem. Eng. Sci.*, 20, 783-84.
- Bowen J.R., 1965, "Comments on the pseudo-steady state approximation for moving boundary problems", *Chem. Eng. Sci.*, 20, 712-13.
- Brandrup J., Immergut E.H. and Grulke E.A., 1999, "Polymer Handbook", New York: Wiley.
- Costantino H.R., Curley J.G. and Hsu C.C., 1997, "Determining the Water Sorption Monolayer of Lyophilized Pharmaceutical Proteins", *J. Pharm. Sci.*, 86(12), 1390-93.
- Crank J., 1979, "The Mathematics of Diffusion", Oxford University Press.
- Gurney H.P. and Lurie J., 1923, "Charts for estimating temperature distributions in Heating or Cooling Solid Shapes", *Ind. Eng. Chem.*, 15(11), 1170-72.

- Hill J.M., 1984, "On the pseudo-steady state approximation for moving boundary diffusion problems", Chem. Eng. Sci., 39, 187-90.
- Howsmon G.J. and Peppas N.A., 1986, "Mathematical Analysis of Transport Properties of Polymer Films for Food Packaging. VI. Coupling of Moisture and Oxygen Transport Using Langmuir Sorption Isotherms", J. Appl. Polym. Sci., 31, 2071-2082.
- IUPAC, 1985, International Union of Pure and Applied Chemistry, "Reporting Physisorption Data for Gas/Solid Systems with Special Reference to the Determination of Surface Area and Porosity", Pure & Appl. Chem., 57(4), 603-619.
- IUPAC, 1994, International Union of Pure and Applied Chemistry, "Recommendations for the Characterization of Porous Solids", *Pure & Appl. Chem.*, 66(8), 1739-1758.
- Karel M., 1967, "Use-tests only real way to determine effect of package on food quality", *Food in Canada*, 43.
- Khanna R. and Peppas N.A., 1978, "Mathematical Analysis of Transport Properties of Flexible Films in Relation to Food Storage Stability: I. Water Vapor Transport", 56-58.
- Khanna R. and Peppas N.A., 1982, "Mathematical Analysis of Transport properties of Polymer Films for Food Packaging. III. Moisture and Oxyegen Diffusion", *AIChE Symp. Series*, 218, 185-191.
- Kim J.N., 1992, "An application of the finite difference method to estimate the shelf life of a packaged moisture sensitive pharmaceutical tablet", Master of Science Thesis, Michigan State University.
- Kim J.N., Hernandez R.J. and Burgess G., 1998, "Modeling the moisture content of a pharmaceutical tablet in a blister package by finite difference method: Program development", J. Plast. Film Sheet., 14, 152-171.
- Labuza T., ca. 1985, "Determination of the Shelf Life of Foods", web site essay, http://faculty.che.umn.edu/fscn/ted_Labuza/PDF_files/papers/General%20Shelf%20Life%20Review.pdf
- Labuza T.P, Mizrahi S., and Karel M., 1972, "Mathematical Models for Optimization of Flexible Film Packaging of Foods for Storage", *Trans. ASAE.*, 15, 150.
- Marsh K.S., Bitner J., David P. and Rao A., 1999, "Shelf Life Prediction Software Finds Application with Ethical Drugs", *Packag. Technol. Sci.*, 12, 173-78.
- Masaro L., Zhu X.X., 1999, "Physical models of diffusion for polymer solutions, gels and solids", *Prog. Polym. Sci.*, 24, 731-775.

- Moreira. R, Vazquez G. and Chenlo F., 2002, "Influence of the temperature on sorption isotherms of chickpea: Evaluation of isoteric heat of sorption", *EJEAFChe.*, 1(1), 1-11.
- Moreira R., Vazquez G., Chenlo. F and Carballal J., 2003 "Desorption isotherms of Eucalyptus Globulus modeling using GAB equation", *EJEAFChe.*, 2(3), 351-55.
- Peppas N.A. and Khanna R., 1980, "Mathematical Analysis of Transport properties of Polymer Films for Food Packaging. II. Generalized Water Vapor Models", *Polym. Eng. Sci.*, 20, 1147-1156.
- Peppas N.A. and Sekhon G.S, 1980, "Mathematical Analysis of Transport Properties of Polymer Films for Food Packaging: IV. Prediction of Shelf-Life of Food Packages Using Halsey Sorption Isotherms", SPE Techn. Papers, ANTEC, 26, 681-684.
- Peppas N.A. and Kline D.F, 1985, "Mathematical Analysis of Transport Properties of Polymer Films for Food Packaging. V. Variable Storage Conditions," *Polym. Mater. Sci. Eng. Prepr.*, 52, 579-583.
- Perry R.H. and Green D.W., 1997, "Perry's Chemical Engineering Handbook", New York: McGraw-Hill.
- Philip J.R., 1994, "Exact solutions for nonlinear diffusion with first-order loss", *Int. J. Heat Mass Tran.*, 37(3), 479-84.
- PQRI, 2005, "Basis for Using Moisture Vapor Transmission Rate Per Unit Product in The Evaluation of Moisture Barrier Equivalence of Primary Packages for Solid Oral Dosage Forms", *Pharmacopeial Forum*, vol 31(1), 2005, web site essay, http://www.pqri.org/pdfs/whitepaper.pdf.
- Rice R.G. and Do D.D., 1995, "Applied Mathematics and Modeling for Chemical Engineers", New York: Wiley.
- Rockland L.B., and Stewart G.F., 1981, "Water Activity: Influences on Food Quality", London: Academic Press.
- Smith J.S. and Peppas N.A., 1991, "Mathematical Analysis of Transport Properties of Polymer Films for Food Packaging" VII. Moisture Transport Through a Polymer Film with Subsequent Adsorption on and Diffusion Through Food, J. Appl. Polym. Sci., 43, 1219-1225.
- Van den Berg C. and Bruin S., 1981, "Water activity and its estimation in food systems: Theoretical aspects", New York, Academic Press.
- Yoon S., 2003, "Designing a package for pharmaceutical tablets in relation to moisture and dissolution", Ph.D. Dissertation, Michigan State University.

Zografi G., Grandolfi G.P., Kontny M.J. and Mendenhall D.W., 1988, "Prediction of moisture transfer in mixtures of solids: transfer via the vapor phase", *Int. J. Pharm.*, 42, 77-88.

